

Influence of Coulomb distortion on polarization observables in elastic electromagnetic hadron lepton scattering at low energies

Hartmuth Arenhövel

Institut für Kernphysik, Johannes Gutenberg-Universität Mainz, D-55099 Mainz, Germany

(Dated: December 18, 2018)

The formal expression for the most general polarization observable in elastic electromagnetic lepton hadron scattering at low energies is derived for the nonrelativistic regime. For the explicit evaluation the influence of Coulomb distortion on various polarization observables is calculated in a distorted wave Born approximation. Besides the hyperfine interaction also the spin-orbit interactions of lepton and hadron are included. For like charges the Coulomb repulsion reduces strongly the size of polarization observables compared to the plane wave Born approximation whereas for opposite charges the Coulomb attraction leads to a substantial increase of these observables for hadron lab kinetic energies below about 20 keV.

PACS numbers: 13.88.+e Polarization in interactions and scattering - 25.30.Bf Elastic electron scattering - 29.27.Hj Polarized beams

I. INTRODUCTION

Recently, Coulomb effects on polarization transfer from polarized electrons or positrons to initially unpolarized protons or antiprotons in elastic electromagnetic scattering have been studied in a distorted wave approximation at low energies [1]. These studies were motivated by the idea to polarize hadrons by their scattering on polarized electrons or positrons in a storage ring [2]. However, in view of such a design it turned out that the considered observable, i.e. the total cross section for the scattering of initially unpolarized hadrons off polarized leptons to polarized final hadrons, the polarization transfer P_{z00z} , cannot contribute to a net polarization of the hadrons in a storage ring. The reason for that is that this polarization observable does not contain a genuine hadronic spin-flip process [3, 4], which is necessary for a net polarization change. Moreover, our previous numerical results were criticized by Milstein et al. [4] who had taken a partial wave expansion of the Coulomb scattering wave function instead of the integral representation used in ref. [1]. Indeed, it turned out that besides a minor error the main reason for the gross overestimation of the polarisation transfer cross section was an accuracy problem in the numerical evaluation, namely, the relevant quantity was calculated as a difference of two almost equal numbers multiplied by a huge factor [5, 6].

For these reasons I have extended the previous study to the formal consideration of all possible polarization observables in this scattering reaction including such spin-flip transitions using again the distorted wave Born approximation. In addition to the previously considered hyperfine interaction I have included also the spin-orbit interactions of lepton and hadron. In the next section the most general scattering cross section is introduced, defining the various polarization observables in terms of bilinear hermitean forms of the T -matrix elements. For the nonrelativistic form of the T -matrix with inclusion of hyperfine and spin-orbit interactions the detailed expression of the general scattering cross section is given, allowing for the polarization of all initial and final particles described by corresponding spin density matrices. In Section III I specialize to the case where the polarization of the final lepton is not measured to the so-called triple polarization cross section. For the numerical evaluation two different methods have been applied, a partial wave expansion as in ref. [4] and an integral representation of the Coulomb wave function according to ref. [7]. Results for the structure functions and spin-flip triple cross sections for the case of polarization along the incoming hadron momentum are presented in Section IV and a summary is given in Section V. Details for the evaluation of the hyperfine and spin-orbit interactions are given in an appendix.

II. THE GENERAL DIFFERENTIAL CROSS SECTION INCLUDING POLARIZATION OF ALL PARTICLES

Reviews on polarization phenomena may be found for lepton hadron scattering in [8], for nuclear physics in [9] and for nucleon nucleon scattering in [10]. I will consider hadron-lepton scattering in the c.m. system, where hadron stands for proton or antiproton and lepton for electron or positron,

$$h(\mathbf{p}) + l(-\mathbf{p}) \longrightarrow h(\mathbf{p}') + l(-\mathbf{p}'), \quad (1)$$

allowing for initial and final hadron and lepton polarization. The hadron initial and final three momenta are denoted by \mathbf{p} and \mathbf{p}' , respectively. All possible observables of this reaction can be obtained from the “quadruple polarization” cross section for which the spin states of all initial and final particles are described by the corresponding general spin density matrices $\rho^{l/h}(\mathbf{P}_{l/h}^{i/f})$, where the initial density matrices characterize the spin properties of target and beam and the final ones those of the detectors. It

is given by the general trace

$$\begin{aligned} \frac{d\sigma_{\mathbf{P}_h^f, \mathbf{P}_h^i, \mathbf{P}_l^f, \mathbf{P}_l^i}^{quadruple}(\theta, \phi)}{d\Omega} &= \mathcal{O}(\mathbf{P}_h^f, \mathbf{P}_l^f, \mathbf{P}_h^i, \mathbf{P}_l^i; \theta, \phi) \\ &= \frac{M_l^2 M_h^2}{\pi^2 W^2 (1 + |\mathbf{P}_l^f|)(1 + |\mathbf{P}_h^f|)} \text{Trace} \left[\widehat{T}^\dagger \widehat{\rho}^h(\mathbf{P}_h^f) \widehat{\rho}^l(\mathbf{P}_l^f) \widehat{T} \widehat{\rho}^h(\mathbf{P}_h^i) \widehat{\rho}^l(\mathbf{P}_l^i) \right], \end{aligned} \quad (2)$$

where $\widehat{T} = \widehat{T}(\theta, \phi)$ denotes the T-matrix of the scattering process with (θ, ϕ) as scattering angles, and $\rho(\mathbf{P})$ the spin density matrix for a spin-1/2 particle, with \mathbf{P} characterizing the polarization of the corresponding particle in the initial and final states, respectively. The trace refers to the hadron and lepton spin degrees of freedom. The factor in front takes into account the final phase space, the incoming flux, and a normalization factor for the case of partially polarized final states. The invariant energy of the hadron-lepton system is denoted by $W = E_h + E_l$ and the masses of hadron and lepton by M_h and M_l , respectively. In the c.m. frame I use as reference system the z -axis along the incoming hadron momentum \mathbf{p} . The x - and y -axes are chosen to form a right handed orthogonal system.

In view of the fact, that in this work I am interested in the low energy regime, a nonrelativistic framework is adopted. The nonrelativistic density matrices for possible polarization of initial and final states of a spin-1/2 particle have the standard form

$$\widehat{\rho}(\mathbf{P}) = \frac{1}{2}(1 + \mathbf{P} \cdot \boldsymbol{\sigma}). \quad (3)$$

with the vector \mathbf{P} describing the polarization of the particle and $\boldsymbol{\sigma}$ denoting the Pauli spin vector. One should note that in general $|\mathbf{P}_{h/l}^{i/f}| \leq 1$.

From the basic equation (2) one obtains all possible polarization observables. In detail they are:

(i) The unpolarized differential cross section:

$$\frac{d\sigma_0(\theta, \phi)}{d\Omega} = \mathcal{O}(\mathbf{0}, \mathbf{0}, \mathbf{0}, \mathbf{0}; \theta, \phi) = S^0(\theta, \phi). \quad (4)$$

(ii) Beam, target and beam-target asymmetries of the differential cross section for unpolarized final states in the notation of Bystricky et al. [10]:

$$\begin{aligned} \frac{d\sigma_{\mathbf{P}_h^i, \mathbf{P}_l^i}(\theta, \phi)}{d\Omega} &= \mathcal{O}(\mathbf{0}, \mathbf{0}, \mathbf{P}_h^i, \mathbf{P}_l^i; \theta, \phi) \\ &= \frac{d\sigma_0(\theta, \phi)}{d\Omega} \left(1 + \sum_j P_{h,j}^i A_{00j0}(\theta, \phi) + \sum_k P_{l,k}^i A_{000k}(\theta, \phi) + \sum_{j,k} P_{h,j}^i P_{l,k}^i A_{00jk}(\theta, \phi) \right), \end{aligned} \quad (5)$$

with the asymmetry vectors

$$\begin{aligned} A_{00j0}(\theta, \phi) &= \frac{1}{S^0} \frac{\partial}{\partial P_{h,j}^i} \mathcal{O}(\mathbf{0}, \mathbf{0}, \mathbf{P}_h^i, \mathbf{0}; \theta, \phi) \\ &= \frac{1}{2S^0} \left(\frac{d\sigma_{\mathbf{P}_h^i, \mathbf{P}_l^i}}{d\Omega} - \frac{d\sigma_{-\mathbf{P}_h^i, \mathbf{P}_l^i}}{d\Omega} \right) \Big|_{P_{h,k}^i = \delta_{jk}}, \end{aligned} \quad (6)$$

$$\begin{aligned} A_{000j}(\theta, \phi) &= \frac{1}{S^0} \frac{\partial}{\partial P_{l,j}^i} \mathcal{O}(\mathbf{0}, \mathbf{0}, \mathbf{0}, \mathbf{P}_l^i; \theta, \phi) \\ &= \frac{1}{2S^0} \left(\frac{d\sigma_{\mathbf{P}_h^i, \mathbf{P}_l^i}}{d\Omega} - \frac{d\sigma_{\mathbf{P}_h^i, -\mathbf{P}_l^i}}{d\Omega} \right) \Big|_{P_{l,k}^i = \delta_{jk}}, \end{aligned} \quad (7)$$

and the hadron-lepton asymmetry tensor

$$\begin{aligned} A_{00jk}(\theta, \phi) &= \frac{1}{S^0} \frac{\partial^2}{\partial P_{h,j}^i \partial P_{l,k}^i} \mathcal{O}(\mathbf{0}, \mathbf{0}, \mathbf{P}_h^i, \mathbf{P}_l^i; \theta, \phi) \\ &= \frac{1}{4S^0} \left(\frac{d\sigma_{\mathbf{P}_h^i, \mathbf{P}_l^i}}{d\Omega} + \frac{d\sigma_{-\mathbf{P}_h^i, -\mathbf{P}_l^i}}{d\Omega} - \frac{d\sigma_{-\mathbf{P}_h^i, \mathbf{P}_l^i}}{d\Omega} - \frac{d\sigma_{\mathbf{P}_h^i, -\mathbf{P}_l^i}}{d\Omega} \right) \Big|_{P_{h,m}^i = \delta_{jm}, P_{l,n}^i = \delta_{kn}}. \end{aligned} \quad (8)$$

(iii) Polarization of the final lepton or hadron for unpolarized beam and target:

$$P_{0j00}(\theta, \phi) = \frac{1}{S^0} \frac{\partial}{\partial P_{l,j}^f} \mathcal{O}(\mathbf{0}, \mathbf{P}_l^f, \mathbf{0}, \mathbf{0}; \theta, \phi), \quad (9)$$

$$P_{j000}(\theta, \phi) = \frac{1}{S^0} \frac{\partial}{\partial P_{h,j}^f} \mathcal{O}(\mathbf{P}_h^f, \mathbf{0}, \mathbf{0}, \mathbf{0}; \theta, \phi). \quad (10)$$

(iv) Various correlations between the polarization of one outgoing particle and beam and/or target polarizations. For example, the outgoing hadron polarization for initial lepton polarization but unpolarized incoming hadron, the lepton-hadron polarization transfer is given by

$$P_{j00k}(\theta, \phi) = \frac{1}{S^0} \frac{\partial^2}{\partial P_{h,j}^f \partial P_{l,k}^i} \mathcal{O}(\mathbf{P}_h^f, \mathbf{0}, \mathbf{0}, \mathbf{P}_l^i; \theta, \phi). \quad (11)$$

(v) Another interesting example is the hadron spin-flip of an initially polarized hadron by the scattering on an initially polarized lepton. It is a special case of the so-called ‘‘triple polarization’’ cross section with all particles polarized except for the final lepton as defined by

$$\frac{d\sigma_{\mathbf{P}_h^f, \mathbf{P}_h^i, \mathbf{P}_l^i}^{triple}(\theta, \phi)}{d\Omega} = \mathcal{O}(\mathbf{P}_h^f, \mathbf{0}, \mathbf{P}_h^i, \mathbf{P}_l^i; \theta, \phi) \quad (12)$$

for the case $\mathbf{P}_h^f = -\mathbf{P}_h^i$, i.e.

$$\frac{d\sigma_{\mathbf{P}_h^i, \mathbf{P}_l^i}^{sf}(\theta, \phi)}{d\Omega} = \frac{d\sigma_{-\mathbf{P}_h^i, \mathbf{P}_h^i, \mathbf{P}_l^i}^{triple}(\theta, \phi)}{d\Omega} = \mathcal{O}(-\mathbf{P}_h^i, \mathbf{0}, \mathbf{P}_h^i, \mathbf{P}_l^i; \theta, \phi). \quad (13)$$

This is the relevant quantity for the method of polarizing hadrons by electromagnetic scattering on polarized leptons in a storage ring [3, 4].

A. The nonrelativistic T -matrix

For the explicit evaluation of the trace in eq. (2) one needs to know the spin dependence of the T -matrix. In a nonrelativistic approach but including contributions of the order M^{-2} , the T -matrix contains the Coulomb, the lepton and hadron spin-orbit and the lepton-hadron hyperfine interactions. Separating the various contributions, the T -matrix is given in an obvious notation by

$$\widehat{T} = \widehat{T}_C + \widehat{T}_{LS_l} + \widehat{T}_{LS_h} + \widehat{T}_{SS}. \quad (14)$$

In detail, one has the Coulomb contribution

$$\widehat{T}_C = 4\pi\alpha a_C, \quad (15)$$

the spin-orbit interactions of lepton and hadron, respectively,

$$\widehat{T}_{LS_{l/h}} = 4\pi\alpha \mathbf{b}_{l/h} \cdot \boldsymbol{\sigma}^{l/h}, \quad (16)$$

and the hyperfine interaction

$$\widehat{T}_{SS} = 4\pi\alpha \boldsymbol{\sigma}^h \cdot \overleftrightarrow{d} \cdot \boldsymbol{\sigma}^l, \quad (17)$$

where \overleftrightarrow{d} denotes a symmetric rank-two tensor, $\mathbf{q} = \mathbf{p}' - \mathbf{p}$ the three-momentum transfer, and α denotes the Sommerfeld fine structure constant. The tensor \overleftrightarrow{d} can be decomposed into a scalar and a spherical tensor of rank two, i.e., a symmetric cartesian tensor with vanishing trace,

$$\overleftrightarrow{d} = d^{[0]} + d^{[2]}, \quad (18)$$

where

$$d_{ij}^{[0]} = d_0 \delta_{ij}, \quad \text{and} \quad d_0 = \frac{1}{3} \text{Trace}(\overleftrightarrow{d}), \quad (19)$$

$$d_{ij}^{[2]} = d_{ij} - d_0 \delta_{ij}. \quad (20)$$

Furthermore, the parameters a_C , $\mathbf{b}_{l/h}$, and \overleftrightarrow{d} depend on what kind of approximation is used. These are:

- (i) Plane wave approximation (PW), corresponding to a pure one-photon exchange; the nonrelativistic reduction of the T -matrix including lowest order relativistic contribution reads

$$\begin{aligned} \widehat{T}^{PW} = & \frac{4\pi\alpha}{q^2} \left\{ Z_l Z_h \left(1 + \frac{\mathbf{P}^2}{4M_l M_h} \right) - \frac{1}{8} \left(Z_h \frac{2\mu_l - 1}{M_l^2} + Z_l \frac{2\mu_h - 1}{8M_h^2} \right) q^2 \right. \\ & - \frac{Z_h}{8M_l} \left(\frac{2\mu_l - 1}{M_l} + \frac{2\mu_l}{M_h} \right) i(\boldsymbol{\sigma}_l \times \mathbf{q}) \cdot \mathbf{P} - \frac{Z_l}{8M_h} \left(\frac{2\mu_h - 1}{M_h} + \frac{2\mu_h}{M_l} \right) i(\boldsymbol{\sigma}_h \times \mathbf{q}) \cdot \mathbf{P} \\ & \left. + \frac{\mu_l \mu_h}{4M_l M_h} (\boldsymbol{\sigma}_l \cdot \mathbf{q} \boldsymbol{\sigma}_h \cdot \mathbf{q} - q^2 \boldsymbol{\sigma}_l \cdot \boldsymbol{\sigma}_h) \right\}, \quad (21) \end{aligned}$$

with $\mathbf{P} = \mathbf{p} + \mathbf{p}'$, Z_l and Z_h as the lepton and hadron charges, and μ_l and μ_h as their magnetic moments, respectively. From this expression one reads off the parameters, keeping in the spin independent term the lowest order only,

$$a_C^{PW} = \frac{Z_l Z_h}{q^2}, \quad (22)$$

$$\mathbf{b}_{l/h}^{PW} = i c_{l/h}^{LS} \frac{\mathbf{P}' \times \mathbf{P}}{q^2}, \quad (23)$$

$$d_{ij}^{PW} = c^{SS} (\widehat{q}_i \widehat{q}_j - \delta_{ij}), \quad (24)$$

where \widehat{q} denotes the unit vector along the three-momentum transfer \mathbf{q} and $q = |\mathbf{q}|$. The separation into a scalar and a traceless tensor according to (18) reads

$$d_0^{PW} = -\frac{2}{3} c^{SS}, \quad (25)$$

$$d_{ij}^{[2]PW} = c^{SS} (\widehat{q}_i \widehat{q}_j - \frac{1}{3} \delta_{ij}). \quad (26)$$

Furthermore, the strength parameters are

$$c_l^{LS} = \frac{Z_h}{4M_l} \left(\frac{2\mu_l - 1}{M_l} + 2 \frac{\mu_l}{M_h} \right), \quad (27)$$

$$c_h^{LS} = \frac{Z_l}{4M_h} \left(\frac{2\mu_h - 1}{M_h} + 2 \frac{\mu_h}{M_l} \right), \quad (28)$$

$$c^{SS} = \frac{\mu_l \mu_h}{4M_l M_h}. \quad (29)$$

One should note that the strength parameter of the hadronic spin-orbit interaction is about three orders of magnitude smaller than the parameter of the leptonic one, because their ratio is approximately

$$\frac{c_h^{LS}}{c_l^{LS}} \approx 2\mu_h \frac{M_l}{M_h} \approx 3 \cdot 10^{-3}. \quad (30)$$

- (ii) Distorted wave approximation (DW) using nonrelativistic Coulomb scattering wave functions

$$\psi_{\mathbf{p}}^{C(+)}(\mathbf{r}) = \sqrt{\frac{\pi\eta_C}{\sinh \pi\eta_C}} e^{-\frac{\pi}{2}\eta_C} e^{i\mathbf{p}\cdot\mathbf{r}} {}_1F_1(-i\eta_C, 1; i(pr - \mathbf{p}\cdot\mathbf{r})) \quad (31)$$

and

$$\psi_{\mathbf{p}}^{C(-)}(\mathbf{r}) = \left(\psi_{-\mathbf{p}}^{C(+)}(\mathbf{r}) \right)^*, \quad (32)$$

where $\psi_{\mathbf{p}}^{C(\pm)}$ denotes the incoming and outgoing scattering waves [11], respectively. Here, ${}_1F_1(a, b; z)$ denotes the confluent hypergeometric function. In the expression for the scattering wave in eq. (31) I have already separated the constant Coulomb phase factor $e^{i\sigma_C}$ with

$$\sigma_C = \arg[\Gamma(1 + i\eta_C)], \quad (33)$$

because it will disappear in the observables. The relevant quantity for Coulomb effects is the Sommerfeld Coulomb parameter

$$\eta_C = \alpha Z_l Z_h / v \quad (34)$$

with v denoting the relative hadron-lepton velocity.

Within this approach one finds

$$a_C^{DW} = e^{i\phi_C} a_C^{PW}, \quad \text{with } \phi_C(\theta) = -\eta_C \ln[\sin^2(\theta/2)], \quad (35)$$

$$\mathbf{b}_{l/h}^{DW} = i \frac{c_{l/h}^{LS}}{4\pi} \int \frac{d^3 r}{r^3} \psi_{\mathbf{p}'}^{C(-)}(\mathbf{r})^* (\mathbf{r} \times \nabla) \psi_{\mathbf{p}}^{C(+)}(\mathbf{r}), \quad (36)$$

$$d_{ij}^{DW} = -\frac{c^{SS}}{4\pi} \int d^3 r \psi_{\mathbf{p}'}^{C(-)}(\mathbf{r})^* \left[\frac{1}{r^3} (3\hat{r}_i \hat{r}_j - \delta_{ij}) + \frac{8\pi}{3} \delta_{ij} \delta(\mathbf{r}) \right] \psi_{\mathbf{p}}^{C(+)}(\mathbf{r}). \quad (37)$$

Separating again the hyperfine contribution into a scalar and a traceless tensor, one obtains

$$d_0^{DW} = -\frac{2}{3} c^{SS} N(\eta_C)^2, \quad (38)$$

$$d_{ij}^{[2]DW} = \frac{c^{SS}}{4\pi} \int \frac{d^3 r}{r^3} \psi_{\mathbf{p}'}^{C(-)}(\mathbf{r})^* (3\hat{r}_i \hat{r}_j - \delta_{ij}) \psi_{\mathbf{p}}^{C(+)}(\mathbf{r}). \quad (39)$$

One should note that the tensor d_{ij}^{DW} in eq. (37) is symmetric as well as $d_{ij}^{[2]DW}$.

B. The general scattering cross section and polarization observables

Evaluation of the trace in eq. (2) yields the following general expression

$$\mathcal{O}(\mathbf{P}_h^f, \mathbf{P}_l^f, \mathbf{P}_h^i, \mathbf{P}_l^i; \theta, \phi) = \sum_{\alpha, \beta \in \{C, LS_l, LS_h, SS\}} S_{\alpha, \beta}(\theta, \phi), \quad (40)$$

where the various contributions are defined by

$$S_{\alpha, \beta}(\theta, \phi) = \frac{M_l^2 M_h^2}{\pi^2 W^2 (1 + |\mathbf{P}_l^f|)(1 + |\mathbf{P}_h^f|)} \text{Trace} \left[\hat{T}_\alpha^\dagger \rho_h^f(\mathbf{P}_h^f) \rho_l^f(\mathbf{P}_l^f) \hat{T}_\beta \rho_h^i(\mathbf{P}_h^i) \rho_l^i(\mathbf{P}_l^i) \right] \quad (41)$$

with \hat{T}_α defined in eqs. (15)-(17). One should note the relation

$$S_{\alpha, \beta} = S_{\beta, \alpha}^*, \quad (42)$$

from which follows that $S_\alpha := S_{\alpha, \alpha}$ is real.

Separating the diagonal contributions (S_α) from the interference terms ($S_{\alpha, \beta}$ for $\alpha \neq \beta$), one obtains for the ‘‘quadruple polarization’’ cross section

$$\frac{d\sigma_{\mathbf{P}_h^f, \mathbf{P}_l^f, \mathbf{P}_h^i, \mathbf{P}_l^i}(\theta, \phi)}{d\Omega} = \sum_{\alpha \in \{C, LS_l, LS_h, SS\}} S_\alpha(\theta, \phi) + \sum_{\alpha < \beta \in \{C, LS_l, LS_h, SS\}} 2 \text{Re } S_{\alpha, \beta}(\theta, \phi). \quad (43)$$

Explicitly, one finds in terms of the different contributions to the T -matrix in eq. (14) for the diagonal terms

$$S_C(\theta, \phi) = V_0 |a_C|^2 \Pi_h^+ \Pi_l^+, \quad (44)$$

$$S_{LS_l}(\theta, \phi) = V_0 \Pi_h^+ \left(\Pi_l^- \mathbf{b}_l^* \cdot \mathbf{b}_l + 2 \operatorname{Re} \left[(\mathbf{b}_l \cdot \mathbf{P}_l^f)^* (\mathbf{b}_l \cdot \mathbf{P}_l^i) \right] \right), \quad (45)$$

$$S_{LS_h}(\theta, \phi) = S_{LS_l}(\theta, \phi)|_{h \leftrightarrow l}, \quad (46)$$

$$\begin{aligned} S_{SS}(\theta, \phi) = & V_0 \left(\Pi_h^- \Pi_l^- D_0 - \mathbf{P}_h^- \cdot \overleftrightarrow{\mathbf{G}} \cdot \mathbf{P}_l^- + \left[\Pi_h^- \mathbf{P}_l^f \cdot \overleftrightarrow{\mathbf{D}} \cdot \mathbf{P}_l^i + (l \leftrightarrow h) \right] \right. \\ & \left. - \operatorname{Im} \left[\left(\Pi_h^- (\mathbf{P}_l^- \cdot \mathbf{H}) + 2 \sum_{jst} P_{l,j}^- P_{h,s}^f P_{h,t}^i E_{jst} \right) + (l \leftrightarrow h) \right] \right. \\ & \left. + 2 \operatorname{Re} \left[(\mathbf{P}_l^f \cdot \overleftrightarrow{\mathbf{d}}^* \cdot \mathbf{P}_h^f) (\mathbf{P}_l^i \cdot \overleftrightarrow{\mathbf{d}} \cdot \mathbf{P}_h^i) + (\mathbf{P}_l^i \cdot \overleftrightarrow{\mathbf{d}}^* \cdot \mathbf{P}_h^f) (\mathbf{P}_h^i \cdot \overleftrightarrow{\mathbf{d}} \cdot \mathbf{P}_l^f) \right] \right), \end{aligned} \quad (47)$$

where

$$V_0 = \frac{4\alpha^2 M_l^2 M_h^2}{W^2 (1 + |\mathbf{P}_l^f|) (1 + |\mathbf{P}_h^f|)}. \quad (48)$$

The following quantities depend on the polarization parameters

$$\Pi_{h/l}^\pm = 1 \pm \mathbf{P}_{h/l}^f \cdot \mathbf{P}_{h/l}^i, \quad (49)$$

$$\mathbf{P}_{h/l}^\pm = \mathbf{P}_{h/l}^i \pm \mathbf{P}_{h/l}^f, \quad (50)$$

$$\mathbf{Q}_{h/l} = \mathbf{P}_{h/l}^+ - i \mathbf{P}_{h/l}^f \times \mathbf{P}_{h/l}^i. \quad (51)$$

Furthermore, I have introduced for convenience the following quantities, which depend on the hyperfine interaction tensor d_{ij} ,

$$D_{ij} = 2 \operatorname{Re} \left(\sum_k d_{ik}^* d_{kj} \right), \quad (52)$$

$$D_0 = \sum_{ij} d_{ij}^* d_{ji} = \frac{1}{2} \operatorname{Trace}(\overleftrightarrow{\mathbf{D}}), \quad (53)$$

$$E_{jst} = \sum_{kl} \varepsilon_{jkl} d_{ks}^* d_{lt}, \quad (54)$$

$$G_{ij} = \sum_{lmst} \varepsilon_{ils} \varepsilon_{jmt} d_{lm}^* d_{st}, \quad (55)$$

$$H_i = \sum_{klm} \varepsilon_{ikl} d_{km}^* d_{ml}, \quad (56)$$

where ε_{ikl} denotes the totally antisymmetric Levi-Civita tensor in three dimensions. These quantities are functions which depend on the scattering angles (θ, ϕ) .

Correspondingly, one finds for the interference terms

$$S_{C,LS_l}(\theta, \phi) = V_0 a_C^* \Pi_h^+ \mathbf{b}_l \cdot \mathbf{Q}_l, \quad (57)$$

$$S_{C,LS_h}(\theta, \phi) = S_{C,LS_l}(\theta, \phi)|_{h \leftrightarrow l}, \quad (58)$$

$$S_{C,SS}(\theta, \phi) = V_0 a_C^* \mathbf{Q}_h \cdot \overleftrightarrow{\mathbf{d}} \cdot \mathbf{Q}_l, \quad (59)$$

$$S_{LS_l,LS_h}(\theta, \phi) = V_0 (\mathbf{b}_l \cdot \mathbf{Q}_l)^* (\mathbf{b}_h \cdot \mathbf{Q}_h), \quad (60)$$

$$S_{LS_l,SS}(\theta, \phi) = V_0 \mathbf{Q}_h \cdot \overleftrightarrow{\mathbf{d}} \cdot \left(\Pi_l^- \mathbf{b}_l^* - i \mathbf{b}_l^* \times \mathbf{P}_l^- + (\mathbf{b}_l^* \cdot \mathbf{P}_l^i) \mathbf{P}_l^f + (\mathbf{b}_l^* \cdot \mathbf{P}_l^f) \mathbf{P}_l^i \right). \quad (61)$$

$$S_{LS_h,SS}(\theta, \phi) = S_{LS_l,SS}(\theta, \phi)|_{h \leftrightarrow l}. \quad (62)$$

Using the separation of the tensor \overleftrightarrow{d} into a scalar and a traceless symmetric tensor according to eq. (18), one finds

$$D_0 = 3|d_0|^2 + \sum_{i,k} d_{ik}^{[2]*} d_{ki}^{[2]}, \quad (63)$$

$$D_{ij} = 2|d_0|^2 \delta_{ij} + 4 \operatorname{Re}(d_0^* d_{ij}^{[2]}) + D_{ij}^{(2)}, \quad (64)$$

$$D_{ij}^{(2)} = 2 \operatorname{Re} \sum_k d_{ik}^{[2]*} d_{kj}^{[2]}, \quad (65)$$

$$E_{jst} = \varepsilon_{jst} |d_0|^2 + \sum_{kl} \varepsilon_{jkl} d_{ks}^{[2]*} d_{lt}^{[2]} + \left(\sum_l \varepsilon_{jst} d_0^* d_{lt}^{[2]} - (s \leftrightarrow t)^* \right), \quad (66)$$

$$G_{ij} = 2|d_0|^2 \delta_{ij} - 2 \operatorname{Re}(d_0^* d_{ij}^{[2]}) + G_{ij}^{(2)}, \quad (67)$$

$$H_i = \sum_{klm} \varepsilon_{ikl} d_{km}^{[2]*} d_{ml}^{[2]}, \quad (68)$$

where

$$G_{ij}^{(2)} = \sum_{lmst} \varepsilon_{ils} \varepsilon_{jmt} d_{lm}^{[2]*} d_{st}^{[2]}. \quad (69)$$

It is now easy to see that the vector \mathbf{H} is purely imaginary and that the tensor G_{ij} is real and symmetric. Furthermore, one notes the symmetry property

$$E_{jst}^* = -E_{jts}. \quad (70)$$

It suffices to evaluate the spin-orbit vector \mathbf{b} and the hyperfine tensor \overleftrightarrow{d} for $\phi = 0$, because then the values for an arbitrary ϕ can be generated by a rotation around the z -axis exploiting their rotation properties. Examples are given in the following section.

III. THE TRIPLE POLARIZATION CROSS SECTION

I will now specialize to the case where only the final lepton polarization is not analyzed, i.e. $\mathbf{P}_l^f = 0$, but all other particles are completely polarized ($|\mathbf{P}_h^{i/f}| = 1$, $|\mathbf{P}_l^i| = 1$). This case is of particular interest for the polarization transfer in a storage ring [3, 4]. The corresponding ‘‘triple polarization’’ cross section has the form

$$\begin{aligned} \frac{d\sigma_{\mathbf{P}_h^f, \mathbf{P}_h^i, \mathbf{P}_l^i}^{triple}(\theta, \phi)}{d\Omega} &= \mathcal{O}(\mathbf{P}_h^f, \mathbf{0}, \mathbf{P}_h^i, \mathbf{P}_l^i; \theta, \phi) \\ &= \sum_{\alpha \in \{C, LS_l, LS_h, SS\}} S_\alpha^{triple}(\theta, \phi) + \sum_{\alpha < \beta \in \{C, LS_l, LS_h, SS\}} 2 \operatorname{Re} S_{\alpha, \beta}^{triple}(\theta, \phi). \end{aligned} \quad (71)$$

In this case, the lepton polarization quantities in (49) through (51) become

$$\Pi_l^\pm = 1, \quad \mathbf{Q}_l = \mathbf{P}_l^i, \quad \mathbf{P}_l^\pm = \mathbf{P}_l^i, \quad (72)$$

and one finds for the diagonal terms

$$S_C^{triple}(\theta) = V \Pi_h^+ |a_C(\theta)|^2, \quad (73)$$

$$S_{LS_l}^{triple}(\theta, \phi) = V \Pi_h^+ \mathbf{b}_l^* \cdot \mathbf{b}_l, \quad (74)$$

$$S_{LS_h}^{triple}(\theta, \phi) = V \left(\Pi_h^- \mathbf{b}_h^* \cdot \mathbf{b}_h + 2 \operatorname{Re} \left[(\mathbf{b}_h \cdot \mathbf{P}_h^f)^* (\mathbf{b}_h \cdot \mathbf{P}_h^i) \right] \right), \quad (75)$$

$$\begin{aligned} S_{SS}^{triple}(\theta, \phi) &= V \left(\Pi_h^- D_0 - \mathbf{P}_h^- \cdot \overleftrightarrow{G} \cdot \mathbf{P}_l^i + \mathbf{P}_h^f \cdot \overleftrightarrow{D} \cdot \mathbf{P}_h^i \right. \\ &\quad \left. - \operatorname{Im} \left[\mathbf{P}_h^- \cdot \mathbf{H} + \Pi_h^- (\mathbf{P}_l^i \cdot \mathbf{H}) + 2 \sum_{jst} P_{l,j}^i P_{h,s}^f P_{h,t}^i E_{jst} \right] \right), \end{aligned} \quad (76)$$

and for the interference terms

$$S_{C,LS_l}^{triple}(\theta, \phi) = V a_C^* \Pi_h^+ \mathbf{b}_l \cdot \mathbf{P}_l^i, \quad (77)$$

$$S_{C,LS_h}^{triple}(\theta, \phi) = V a_C^* \mathbf{b}_h \cdot \mathbf{Q}_h, \quad (78)$$

$$S_{C,SS}^{triple}(\theta, \phi) = V a_C^* \mathbf{Q}_h \cdot \overleftrightarrow{d} \cdot \mathbf{P}_l^i, \quad (79)$$

$$S_{LS_l,LS_h}^{triple}(\theta, \phi) = V (\mathbf{b}_l \cdot \mathbf{P}_l^i)^* (\mathbf{b}_h \cdot \mathbf{Q}_h), \quad (80)$$

$$S_{LS_l,SS}^{triple}(\theta, \phi) = V \mathbf{Q}_h \cdot \overleftrightarrow{d} \cdot (\mathbf{b}_l^* - i \mathbf{b}_l^* \times \mathbf{P}_l^i), \quad (81)$$

$$S_{LS_h,SS}^{triple}(\theta, \phi) = V \mathbf{P}_l^i \cdot \overleftrightarrow{d} \cdot (\Pi_h^- \mathbf{b}_h^* - i \mathbf{b}_h^* \times \mathbf{P}_h^- + (\mathbf{b}_h^* \cdot \mathbf{P}_h^i) \mathbf{P}_h^f + (\mathbf{b}_h^* \cdot \mathbf{P}_h^f) \mathbf{P}_h^i). \quad (82)$$

where

$$V = \frac{2\alpha^2 M_l^2 M_h^2}{W^2}. \quad (83)$$

From now on as a further specialization, I will consider only polarization along the incoming direction which is chosen as z -axis. Then with

$$\mathbf{P}_h^{i/f} = \lambda_h^{i/f} \hat{z}, \quad \mathbf{P}_h^\pm = (\lambda_h^i \pm \lambda_h^f) \hat{z}, \quad \text{and} \quad \Pi_h^\pm = 1 \pm \lambda_h^i \lambda_h^f, \quad (84)$$

where $\lambda_h^\pm = \lambda_h^i \pm \lambda_h^f$, one obtains

$$\begin{aligned} \frac{d\sigma_{\lambda_h^f, \lambda_h^i, \lambda_l^i}^{triple}(\theta, \phi)}{d\Omega} &= (1 + \lambda_h^i \lambda_h^f) \left[S_C(\theta) + S_0(\theta, \phi) + L_0^l(\theta, \phi) \right] + (1 - \lambda_h^i \lambda_h^f) \left[L_0^h(\theta, \phi) + \lambda_l^i \left(S_1(\theta, \phi) + L_1^h(\theta, \phi) \right) \right] \\ &+ \lambda_h^- \left[S_1(\theta, \phi) + \lambda_l^i \left(S_2^-(\theta, \phi) + L_2^h(\theta, \phi) \right) \right] + \lambda_h^+ \left[\lambda_l^i \left(S_2^+(\theta, \phi) + L_2^l(\theta, \phi) \right) + L_1^l(\theta, \phi) \right] \\ &+ \lambda_h^i \lambda_h^f \left[S_2(\theta, \phi) + \lambda_l^i S_3(\theta, \phi) \right]. \end{aligned} \quad (85)$$

The diagonal contributions are

$$L_0^{l/h}(\theta, \phi) = V |\mathbf{b}_{l/h}(\theta, \phi)|^2, \quad (86)$$

$$S_C(\theta) = V |a_C|^2, \quad (87)$$

$$S_0(\theta, \phi) = V \left(3|d_0|^2 + \sum_j D_{jj}(\theta, \phi) \right), \quad (88)$$

$$S_1(\theta, \phi) = iV \sum_{jk} \epsilon_{3jk} D_{jk}(\theta, \phi) = i(D_{12}(\theta, \phi) - D_{21}(\theta, \phi)) = -2 \text{Im}(D_{12}(\theta, \phi)), \quad (89)$$

$$S_2^-(\theta, \phi) = 2V \left(\text{Re} \left(d_0^* d_{33}^{[2]}(\theta, \phi) - d_{11}^{[2]}(\theta, \phi)^* d_{22}^{[2]}(\theta, \phi) \right) - |d_0|^2 + |d_{12}^{[2]}(\theta, \phi)|^2 \right), \quad (90)$$

$$S_2(\theta, \phi) = 2V \left(2 \text{Re} \left(d_0^* d_{33}^{[2]}(\theta, \phi) \right) - 2|d_0|^2 - D_{11}(\theta, \phi) - D_{22}(\theta, \phi) \right), \quad (91)$$

$$S_3(\theta, \phi) = -4V \text{Im} \left(d_{31}^{[2]}(\theta, \phi)^* d_{32}^{[2]}(\theta, \phi) \right), \quad (92)$$

and the interference terms

$$L_1^{l/h}(\theta, \phi) = 2V \text{Re} \left(d_{31}^{[2]}(\theta, \phi) b_{l/h,1}^*(\theta, \phi) + d_{32}^{[2]}(\theta, \phi) b_{l/h,2}^*(\theta, \phi) \right), \quad (93)$$

$$L_2^{l/h}(\theta, \phi) = 2V \text{Im} \left(d_{31}^{[2]}(\theta, \phi) b_{l/h,2}^*(\theta, \phi) - d_{32}^{[2]}(\theta, \phi) b_{l/h,1}^*(\theta, \phi) \right), \quad (94)$$

$$S_2^+(\theta, \phi) = 2V \text{Re} \left[a_C^* (d_0 + d_{33}^{[2]}(\theta, \phi)) \right]. \quad (95)$$

Here I have already used the fact that the spin-orbit vector $\mathbf{b}_{l/h}$ is perpendicular to the z -axis, i.e. its third component vanishes. Indeed, as shown explicitly in the appendix, it has the form

$$\mathbf{b}_{l/h}(\theta, \phi) = i b_0^{l/h}(\theta) (-\sin \phi, \cos \phi, 0) = i b_0^{l/h}(\theta) \frac{\mathbf{p}' \times \mathbf{p}}{|\mathbf{p}' \times \mathbf{p}|}. \quad (96)$$

However, not all of the contributions in eqs. (86) through (95) are nonzero. In fact, I now will show that the diagonal contributions S_1 and S_3 and the interference terms $L_1^{l/h}$ vanish identically. To this end I first will consider the ϕ -dependence of the tensors $d^{[2]}(\theta, \phi)$ and $D(\theta, \phi)$. It suffices to evaluate them for $\phi = 0$ from which one obtains $d^{[2]}(\theta, \phi)$ and $D(\theta, \phi)$ by a rotation around the z -axis by an angle ϕ . Introducing the notation $d^{[2],0}(\theta) = d^{[2]}(\theta, \phi = 0)$ and correspondingly $D^0 = D(\theta, 0)$, and using furthermore the fact $d_{12}^{[2],0} = d_{21}^{[2],0} = 0$, one finds

$$d^{[2]}(\theta, \phi) = \begin{pmatrix} d_{11}^{[2],0}(\theta) \cos^2 \phi + d_{22}^{[2],0}(\theta) \sin^2 \phi & \frac{1}{2}(d_{11}^{[2],0}(\theta) - d_{22}^{[2],0}(\theta)) \sin 2\phi & d_{13}^{[2],0}(\theta) \cos \phi \\ \frac{1}{2}(d_{11}^{[2],0}(\theta) - d_{22}^{[2],0}(\theta)) \sin 2\phi & d_{11}^{[2],0}(\theta) \sin^2 \phi + d_{22}^{[2],0}(\theta) \cos^2 \phi & d_{13}^{[2],0}(\theta) \sin \phi \\ d_{13}^{[2],0}(\theta) \cos \phi & d_{13}^{[2],0}(\theta) \sin \phi & d_{33}^{[2],0}(\theta) \end{pmatrix}. \quad (97)$$

From this representation one notes immediately that

$$d_{31}^{[2]}(\theta, \phi) * d_{32}^{[2]}(\theta, \phi) = |d_{13}^{[2],0}(\theta)| \cos \phi \sin \phi \quad (98)$$

is real and thus $S_3(\theta, \phi) = 0$ according to eq. (92). Furthermore, with

$$D^0(\theta) = \begin{pmatrix} |d_{11}^{[2],0}(\theta)|^2 + |d_{13}^{[2],0}(\theta)|^2 & 0 & d_{11}^{[2],0}(\theta) * d_{13}^{[2],0}(\theta) + d_{13}^{[2],0}(\theta) * d_{33}^{[2],0}(\theta) \\ 0 & |d_{22}^{[2],0}(\theta)| & 0 \\ d_{13}^{[2],0}(\theta) * d_{11}^{[2],0}(\theta) + d_{33}^{[2],0}(\theta) * d_{13}^{[2],0}(\theta) & 0 & |d_{33}^{[2],0}(\theta)|^2 + |d_{13}^{[2],0}(\theta)|^2 \end{pmatrix}, \quad (99)$$

which formally has the same structure as $d^{[2],0}(\theta)$, one finds

$$D(\theta, \phi) = \begin{pmatrix} D_{11}^0(\theta) \cos^2 \phi + D_{22}^0(\theta) \sin^2 \phi & \frac{1}{2}(D_{11}^0(\theta) - D_{22}^0(\theta)) \sin 2\phi & D_{13}^0(\theta) \cos \phi \\ \frac{1}{2}(D_{11}^0(\theta) - D_{22}^0(\theta)) \sin 2\phi & D_{11}^0(\theta) \sin^2 \phi + D_{22}^0(\theta) \cos^2 \phi & D_{13}^0(\theta) \sin \phi \\ D_{13}^0(\theta) \cos \phi & D_{13}^0(\theta) \sin \phi & D_{33}^0(\theta) \end{pmatrix}. \quad (100)$$

Here again one notes that

$$D_{12}(\theta, \phi) = \frac{1}{2}(D_{11}^0(\theta) - D_{22}^0(\theta)) \sin 2\phi \quad (101)$$

is real because according to eq. (99) $D_{11}^0(\theta)$ and $D_{22}^0(\theta)$ are real and, therefore, $S_1 = 0$. For the spin-orbit interaction vector $\mathbf{b}_{l/h}$ one finds from eq. (96) $|\mathbf{b}_{l/h}(\theta, \phi)|^2 = |b_0^{l/h}(\theta)|^2$, which means that $L_0^{l/h}$ is ϕ -independent. Moreover, using eqs. (96) and (97) one obtains

$$L_1^{l/h}(\theta, \phi) = 4V \operatorname{Re} \left(d_{13}^{[2],0}(\theta) \cos \phi (-b_0^{l/h}(\theta) \sin \phi) + d_{13}^{[2],0}(\theta) \sin \phi b_0^{l/h}(\theta) \cos \phi \right) = 0. \quad (102)$$

Finally, with the help of eqs. (97) through (100) one finds that the remaining structure functions become ϕ -independent, which is easy to understand since all polarizations are assumed to be along the z -axis ruling out any ϕ -dependence. Thus also the cross section simplifies to

$$\begin{aligned} \frac{d\sigma_{\lambda_h^f, \lambda_h^i, \lambda_l^i}^{triple}}{d\Omega} &= (1 + \lambda_h^i \lambda_h^f) \left[S_C(\theta) + S_0(\theta) + L_0^l(\theta) \right] + (1 - \lambda_h^i \lambda_h^f) L_0^h(\theta) \\ &\quad + \lambda_l^i \left[\lambda_h^- \left(S_2^-(\theta, \phi) + L_2^h(\theta) \right) + \lambda_h^+ \left(S_2^+(\theta) + L_2^l(\theta) \right) \right] + \lambda_h^i \lambda_h^f S_2(\theta), \end{aligned} \quad (103)$$

where the structure functions are given by

$$L_0^{l/h}(\theta) = V|b_0^{l/h}(\theta)|^2, \quad (104)$$

$$L_2^{l/h}(\theta) = 2V \operatorname{Re} \left[d_{13}^{[2],0}(\theta) b_0^{l/h}(\theta)^* \right], \quad (105)$$

$$S_0(\theta) = V \left(3|d_0|^2 + \sum_{j=1}^3 |d_{jj}^{[2],0}(\theta)|^2 + 2|d_{13}^{[2],0}(\theta)|^2 \right), \quad (106)$$

$$S_2^+(\theta) = 2V \operatorname{Re} \left[a_C^* \left(d_0 + d_{33}^{[2],0}(\theta) \right) \right], \quad (107)$$

$$S_2^-(\theta) = 2V \left[\operatorname{Re} \left(d_0^* d_{33}^{[2],0}(\theta) - d_{11}^{[2],0}(\theta)^* d_{22}^{[2],0}(\theta) \right) - |d_0|^2 \right], \quad (108)$$

$$S_2(\theta) = 2V \left[2 \operatorname{Re} \left(d_0^* d_{33}^{[2],0}(\theta) \right) - 2|d_0|^2 - |d_{11}^{[2],0}(\theta)|^2 - |d_{22}^{[2],0}(\theta)|^2 - |d_{13}^{[2],0}(\theta)|^2 \right]. \quad (109)$$

The expression in eq. (103) is an extension of the triple polarization cross section given in eq. (16) of ref. [3] by including the contributions from the hadron and lepton spin-orbit interactions. (As a sideremark: The corresponding cross section for final lepton polarization is obtained from (85) by the substitutions $\lambda_h^f \rightarrow \lambda_l^f$ and $\lambda_h^i \leftrightarrow \lambda_l^i$.)

As a special case, one considers the so-called hadronic spin-flip cross section for complete hadron polarization, i.e. $\lambda_h^i = -\lambda_h^f = \lambda_h = \pm 1$, and the non-spin-flip cross section with $\lambda_h^i = \lambda_h^f = \lambda_h = \pm 1$. For the spin-flip cross section one finds

$$\frac{d\sigma_{-\lambda_h, \lambda_h, \lambda_l^i}^{\text{sf}}(\theta, \phi)}{d\Omega} = 2L_0^h(\theta) - S_2(\theta) + 2\lambda_l^i \lambda_h \left[S_2^-(\theta, \phi) + L_2^h(\theta) \right]. \quad (110)$$

It is governed by the hyperfine terms S_2 and S_2^- and the hadronic spin-orbit interaction via L_0^h and L_2^h . On the other hand, the non-spin-flip cross section is given by

$$\frac{d\sigma_{\lambda_h, \lambda_h, \lambda_l^i}^{\text{nsf}}(\theta, \phi)}{d\Omega} = 2 \left[S_C(\theta) + S_0(\theta) + L_0^l(\theta) \right] + S_2(\theta) + 2\lambda_l^i \lambda_h \left[S_2^+(\theta, \phi) + L_2^l(\theta) \right]. \quad (111)$$

Its helicity independent part is overwhelmingly dominated by the Coulomb term S_C with additional tiny contributions from the hyperfine and the leptonic spin-orbit interactions. The difference of the non-spin-flip cross section for $\lambda_h = \pm 1$

$$\frac{1}{2} \left(\frac{d\sigma_{1,1,\lambda}^{\text{nsf}}(\theta, \phi)}{d\Omega} - \frac{d\sigma_{-1,-1,\lambda}^{\text{nsf}}(\theta, \phi)}{d\Omega} \right) = 2\lambda \left[S_2^+(\theta, \phi) + L_2^l(\theta) \right] \quad (112)$$

has been considered as lepton-hadron polarization transfer in [2]. This polarization transfer is dominated by the hyperfine structure function S_2^+ because the additional spin-orbit contribution L_2^l is comparably small as shown in the next section. It differs by a factor 2 and the presence of L_2^l from the polarization transfer P_{z00z} for the scattering of unpolarized hadrons on polarized leptons as considered in ref. [1], where I had considered only the leading term S_2^+ , the interference between Coulomb and hyperfine amplitudes, neglecting higher order contributions. The more complete expression reads

$$\begin{aligned} P_{z00z} \frac{d\sigma_0(\theta, \phi)}{d\Omega} &= \frac{\partial^2}{\partial \lambda_h^f \partial \lambda_l^i} \frac{d\sigma_{\lambda_h^f, \lambda_h^i, \lambda_l^i}^{\text{triple}}(\theta, \phi)}{d\Omega} \Big|_{\lambda_h^i=0} \\ &= S_2^+(\theta, \phi) - S_2^-(\theta, \phi) + L_2^l(\theta, \phi) - L_2^h(\theta, \phi). \end{aligned} \quad (113)$$

In addition to S_2^+ , it includes S_2^- , which is quadratic in the hyperfine amplitude, and L_2^l and L_2^h , the contributions from the interference of hyperfine and leptonic and hadronic spin-orbit amplitudes, respectively. However, the largest of these additional terms, L_2^l , is still quite small if not negligible compared to S_2^+ .

IV. RESULTS FOR STRUCTURE FUNCTIONS AND POLARIZATION CROSS SECTIONS

For the evaluation of the structure functions in eq. (103) and the corresponding cross section I have used both methods for the calculation of Coulomb distortion, the integral representation as well as the partial wave expansion. The integral representation has been used mainly in order to check the convergence of the partial wave expansion as is described in detail in the appendix. Thus all results presented in this section are based on the partial wave expansion (PWE). For the hyperfine amplitude it was found that an expansion up to a partial wave with $l_{max} = 2000$ was sufficient, but for the spin-orbit interaction, being much slower convergent, $l_{max} = 4000$ was taken.

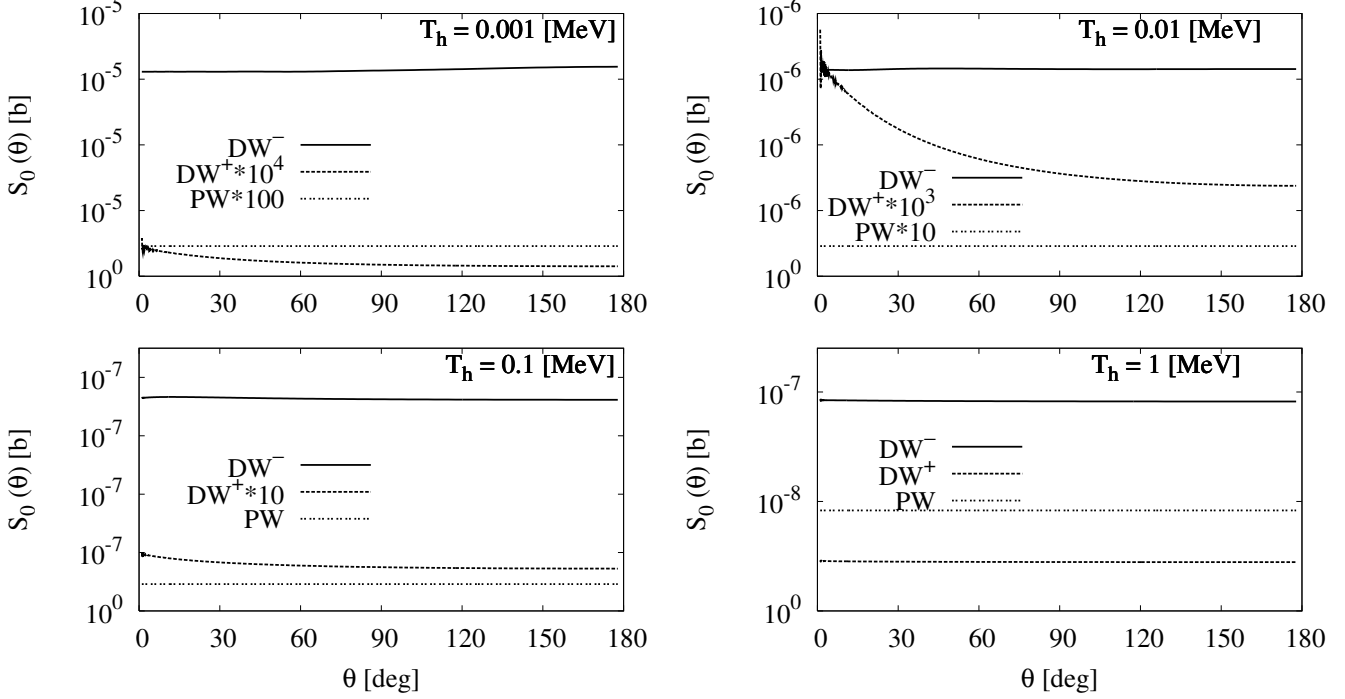


FIG. 1: Structure function $S_0(\theta)$ of the triple polarization differential cross section in plane wave (PW) and distorted wave approximation for like charges (DW^+) and opposite charges (DW^-) for various proton lab kinetic energies T_h .

A. The structure functions

First, I will discuss the various structure functions which determine the triple polarization cross section of eq. (103). For the plane wave approximation, one finds easily the following expressions

$$L_0^{l/h}(\theta) = -\frac{1}{4} V (c_{l/h}^{LS})^2 \cot^2(\theta/2), \quad (114)$$

$$L_2^{l/h}(\theta) = -V c_{l/h}^{LS} c^{SS} \cos^2(\theta/2), \quad (115)$$

$$S_0(\theta) = 2 V (c^{SS})^2, \quad (116)$$

$$S_2^+(\theta) = -\frac{V c^{SS}}{2p^2} \cot^2(\theta/2), \quad (117)$$

$$S_2^-(\theta) = -2 V (c^{SS})^2 \sin^2(\theta/2), \quad (118)$$

$$S_2(\theta) = -2 V (c^{SS})^2 (1 + \sin^2(\theta/2)). \quad (119)$$

The structure functions, evaluated in the c.m. frame for several lab kinetic energies, are shown in Figs. 1 through 6 for the various approximations, i.e. plane wave approximation (PW) and Coulomb distortion for like (DW^+) and opposite charges (DW^-).

The diagonal structure function S_0 in Fig. 1, induced by the hyperfine interaction, shows a rather flat, almost constant angular behaviour. Its size scales roughly proportional to the inverse of the kinetic energy T_h . Compared to the plane wave approximation (PW), the distorted wave approximation is strongly enhanced for unlike charges (DW^-) and strongly suppressed for like charges (DW^+) by several orders of magnitude for the lowest lab kinetic energy of $T_h = 0.001$ MeV corresponding to $\eta_C \approx 5$. This enhancement resp. suppression is increasingly reduced with growing kinetic energy T_h and approaches the plane wave result above $T_h = 10$ MeV. The pure Coulomb contribution S_C , however, is much larger by more than ten orders of magnitude.

With respect to the other two diagonal structure functions from the leptonic and hadronic spin-orbit interactions L_0^l and L_0^h , it suffices to show only the former one in Fig. 2, because L_0^h differs in magnitude only by the factor $(c_{LS}^h/c_{LS}^l)^2$ being smaller by about five orders of magnitude. One readily notes that L_0^l exhibits a strong peaking in the forward direction only and tends to oscillate at small angles for the lowest T_h considered here. Over the whole angular range, especially in the forward direction, L_0^l is much larger by several orders of magnitude than S_0 but it is still almost negligible compared to the size of S_C . The effect of Coulomb distortion is qualitatively similar to what one observes in S_0 .

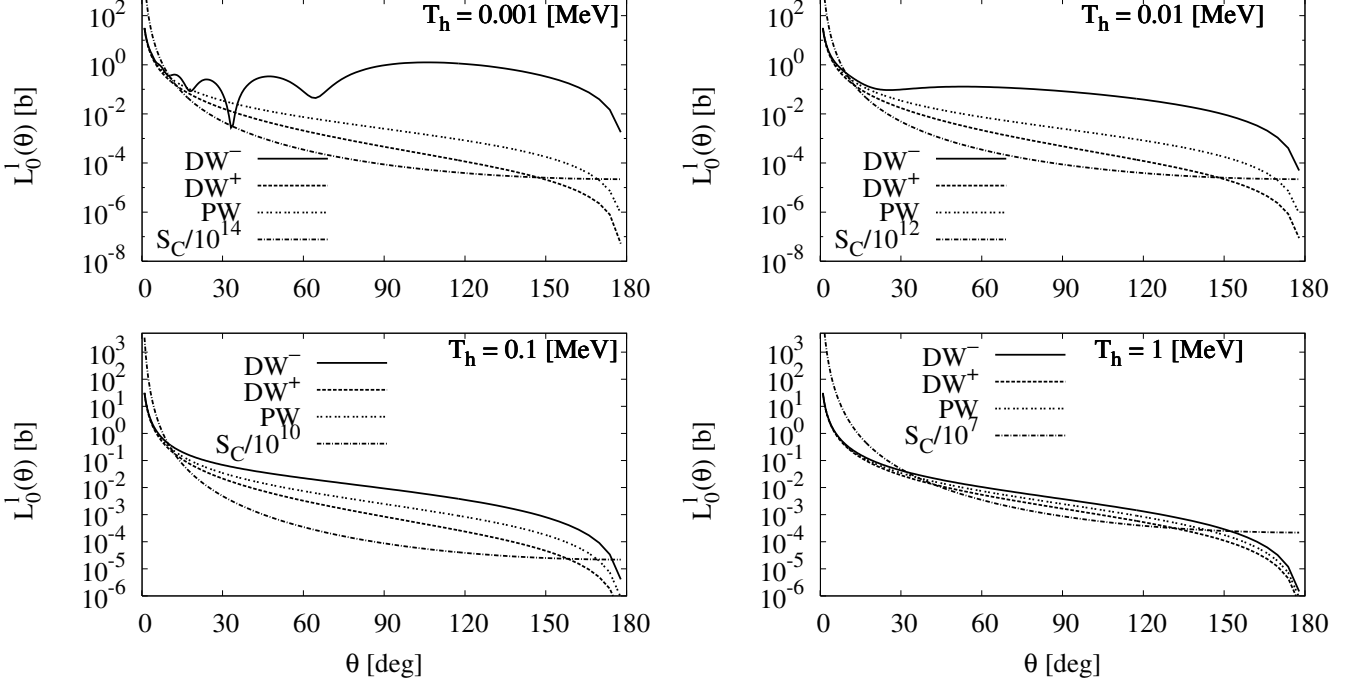


FIG. 2: The structure function $L_0^l(\theta)$ of the triple polarization differential cross section in plane wave (PW) and distorted wave approximation for like charges (DW⁺) and opposite charges (DW⁻) for various proton lab kinetic energies T_h . For comparison the Coulomb structure function $S_C(\theta)$ is shown in addition reduced by a factor 10^{-n} .

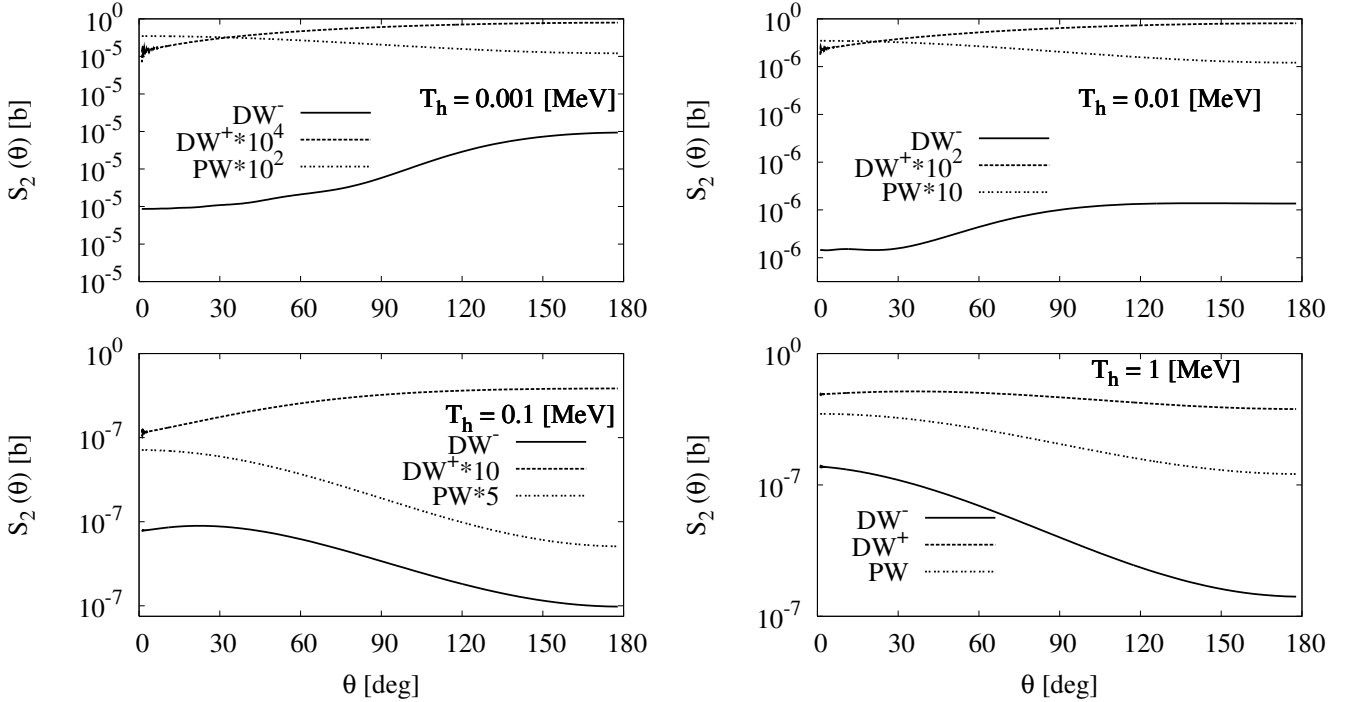


FIG. 3: The structure function $S_2(\theta)$ of the triple polarization differential cross section in plane wave (PW) and distorted wave approximation for like charges (DW⁺) and opposite charges (DW⁻) for various proton lab kinetic energies T_h . One should note the enhancement factors for PW and DW⁺.

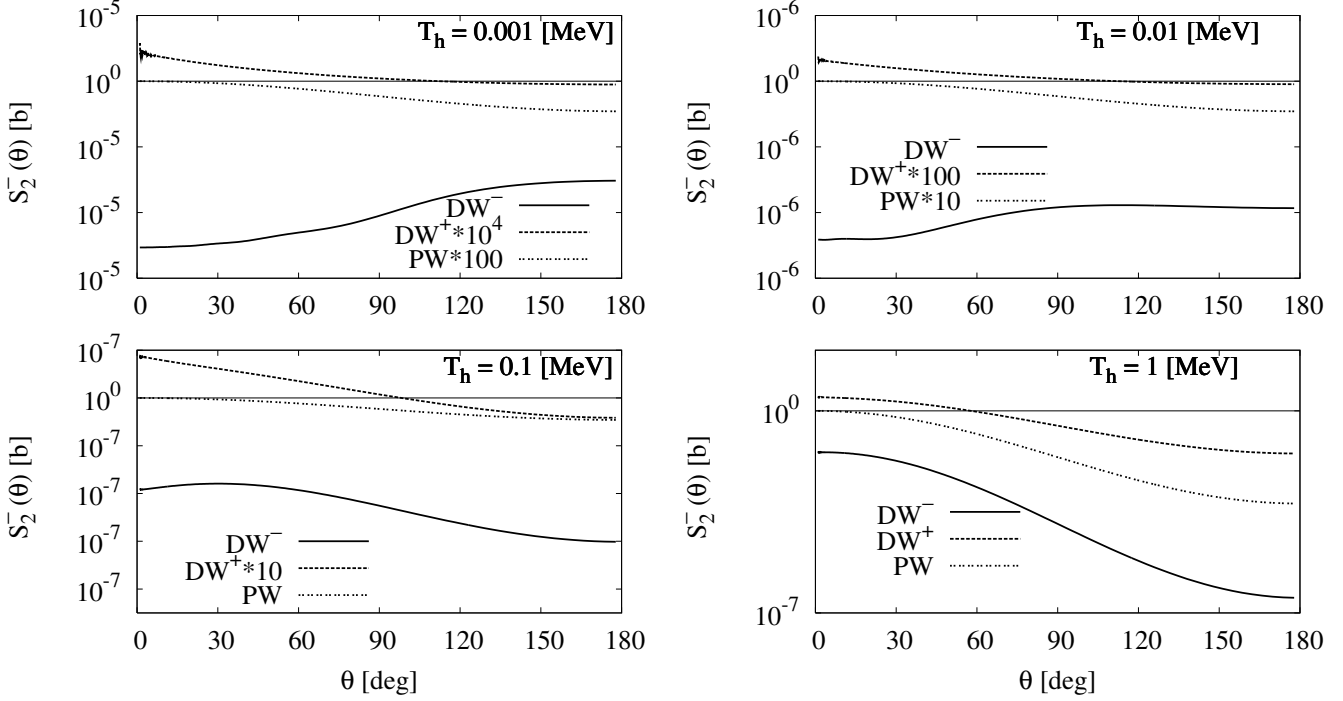


FIG. 4: The structure function $S_2^-(\theta)$ of the triple polarization differential cross section in plane wave (PW) and distorted wave approximation for like charges (DW^+) and opposite charges (DW^-) for various proton lab kinetic energies T_h . One should note the enhancement factors for PW and DW^+ .

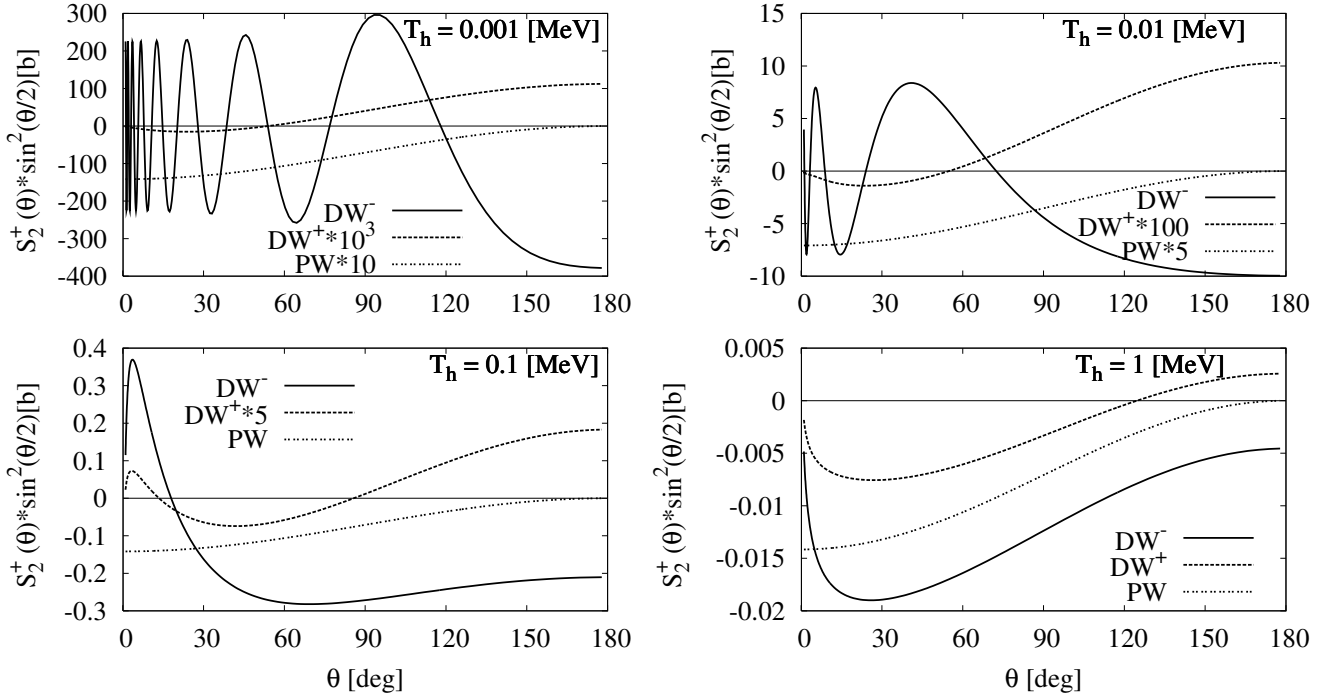


FIG. 5: The structure function $S_2^+(\theta)$ of the triple polarization differential cross section scattering multiplied by $\sin^2(\theta/2)$ in plane wave (PW) and distorted wave approximation for like charges (DW^+) and opposite charges (DW^-) for various proton lab kinetic energies T_h . One should note the enhancement factors for PW and DW^+ .

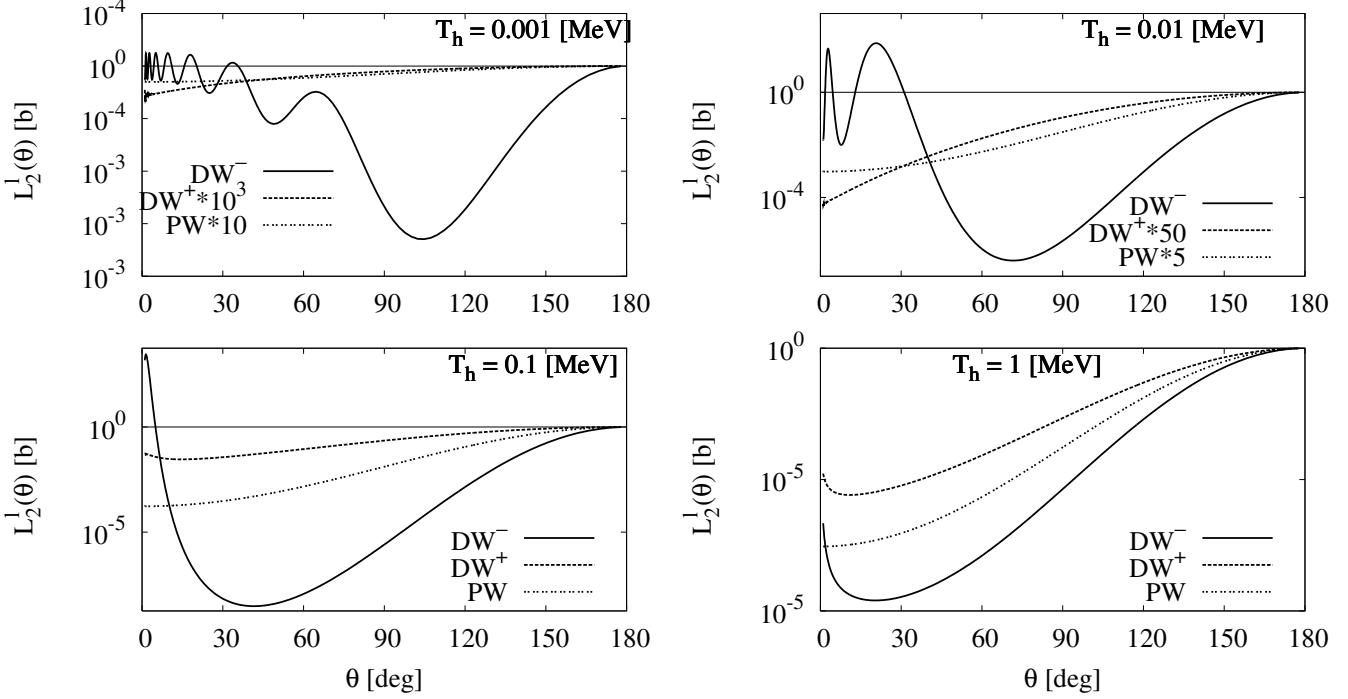


FIG. 6: The structure function $L_2^l(\theta)$ of the triple polarization differential cross section in plane wave (PW) and distorted wave approximation for like charges (DW^+) and opposite charges (DW^-) for various proton lab kinetic energies T_h . One should note the enhancement factors for PW and DW^+ in the upper panels.

Only these diagonal structure functions contribute to the unpolarized cross section. However, as already mentioned, their relative contribution is extremely small as can be seen by comparison with the pure Coulomb structure function S_C which is also shown in Fig. 2 indicated by the large reduction factor applied to S_C .

The two hyperfine-hyperfine interference structure functions S_2 and S_2^- , shown in Figs. 3 and 4, which both are negative throughout, exhibit a similar pattern, a smooth angular distribution with a slight decrease in size at backward angles for the two lowest kinetic energies, but with a slight increase for the two higher kinetic energies like the PW result for all four cases. Again one notes sizeable enhancements for opposite charges by Coulomb distortion and suppression for like charges for the lowest energies T_h . The distortion effect decreases with increasing T_h . Also these two structure functions are quite small like S_0 because they are quadratic in the hyperfine amplitudes.

Much larger is the third interference structure function S_2^+ because it is an interference between the Coulomb and the hyperfine amplitudes. Thus it is strongly forward peaked. For this reason, it is displayed in Fig. 5 multiplied by $\sin^2(\theta/2)$. Moreover, Coulomb distortion induces a strong oscillatory behavior, again in conjunction with a large enhancement for opposite charges and strong suppression for like charges. As expected, the distortion effect diminishes with increasing kinetic energy T_h . I would like to point out that in the corresponding Figs. 1 and 2 of ref. [1] erroneously a factor $\sin^2(2\theta)$ instead of the indicated factor $\sin^2(\theta/2)$ has been applied.

Finally, the spin-orbit-hyperfine interference structure function L_2^l in Fig. 6 is comparable in size to S_2 and S_2^- but exhibits quite a different pattern. At the lowest kinetic energy T_h it is strongly enhanced by distortion for opposite charges and possesses a pronounced broad minimum around 100° . It falls off at forward and backward angles with many oscillations in the forward direction. With increasing kinetic energy the minimum moves towards smaller angles with fewer oscillations. Again the distortion effect decreases strongly with increasing energy. Like the diagonal structure function L_0^h , the hadronic interference structure function L_2^h is quite negligible.

B. The triple polarization cross section

Now I will discuss the triple polarization cross section of eq. (103). Previously, in ref. [3] only the hyperfine amplitude besides the Coulomb one has been considered, whereas the hadron spin-orbit interaction has been included already in ref. [4]. However, as mentioned above, its contribution to the helicity dependent part of the spin-flip cross section in eq. (110) is negligible, whereas in the helicity independent part the diagonal contribution L_0^h is comparable in size to S_2 in the forward direction (compare Figs. 2

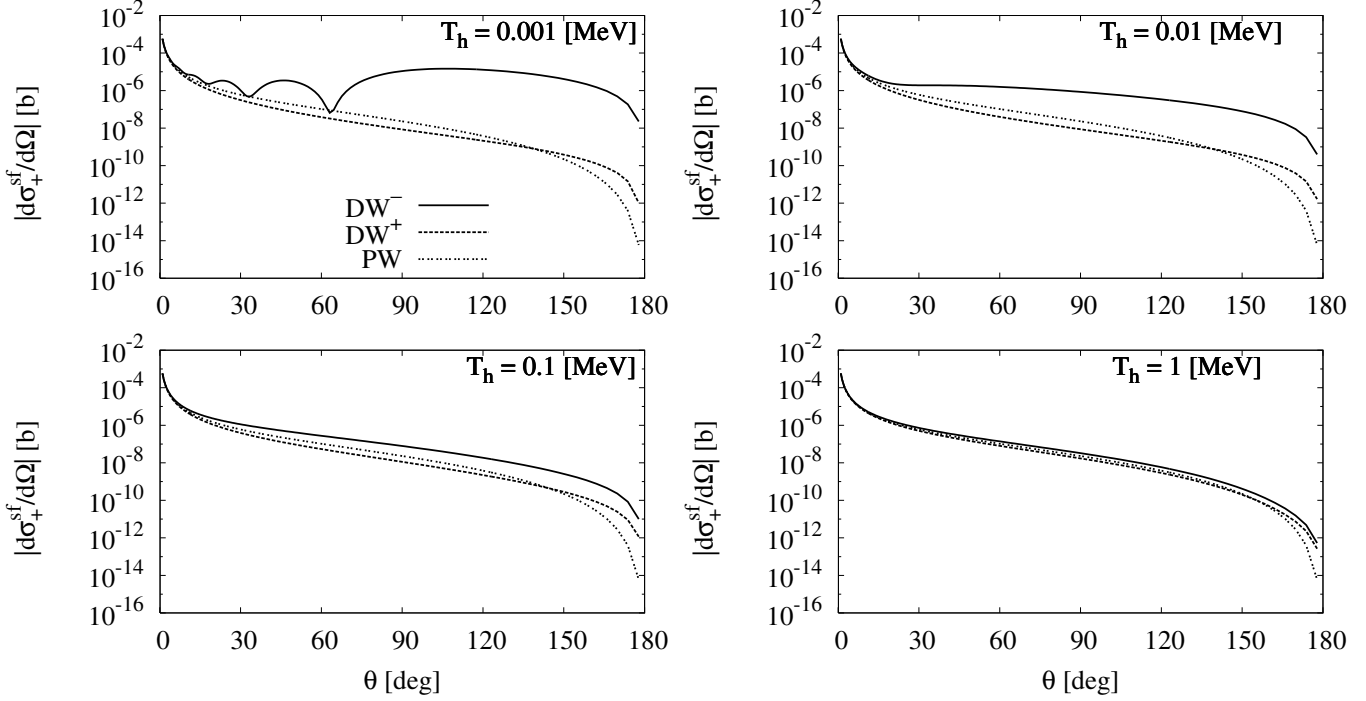


FIG. 7: Absolute value of spin-flip cross section $d\sigma_+^{sf}/d\Omega$ for initial hadron polarization parallel to lepton polarization along the initial relative momentum in plane wave (PW) and distorted wave approximation for like charges (DW^+) and opposite charges (DW^-) for various proton lab kinetic energies T_h .

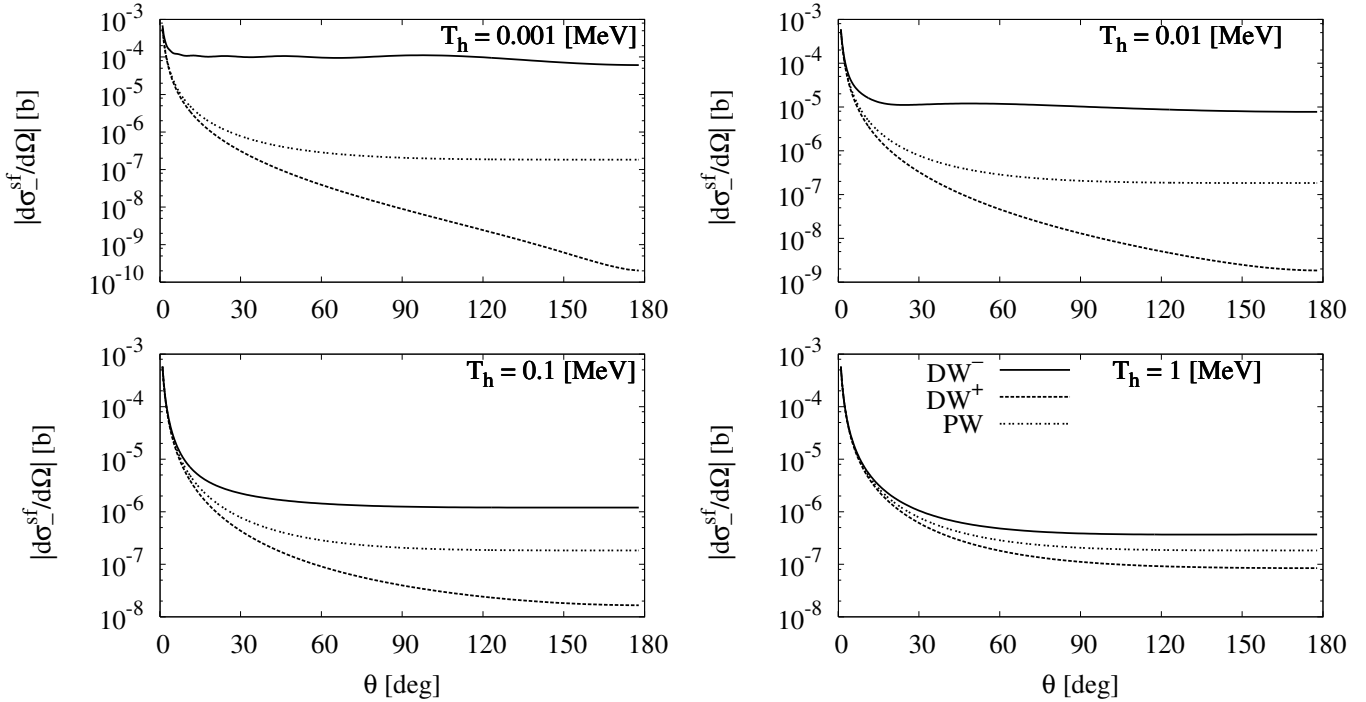


FIG. 8: Absolute value of spin-flip cross section $d\sigma_-^{sf}/d\Omega$ for initial hadron polarization opposite to lepton polarization along the initial relative momentum in plane wave (PW) and distorted wave approximation for like charges (DW^+) and opposite charges (DW^-) for various proton lab kinetic energies T_h .

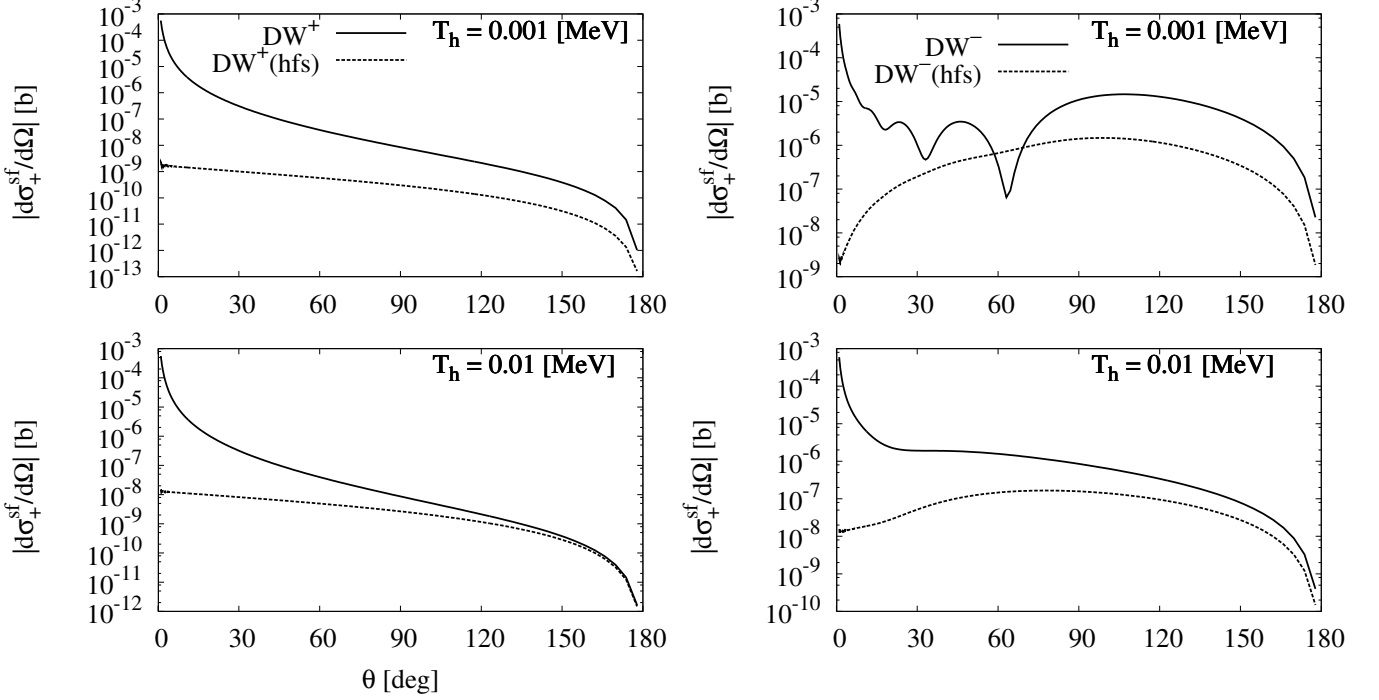


FIG. 9: Comparison of spin-flip cross section $d\sigma_+^{sf}/d\Omega$ for initial hadron polarization parallel to lepton polarization along the initial relative momentum with the hyperfine interaction alone (DW(hfs)) and with inclusion of the spin-orbit contribution (DW) for like charges (DW^+ , left panels) and opposite charges (DW^- , right panels) for the two lowest proton lab kinetic energies T_h .

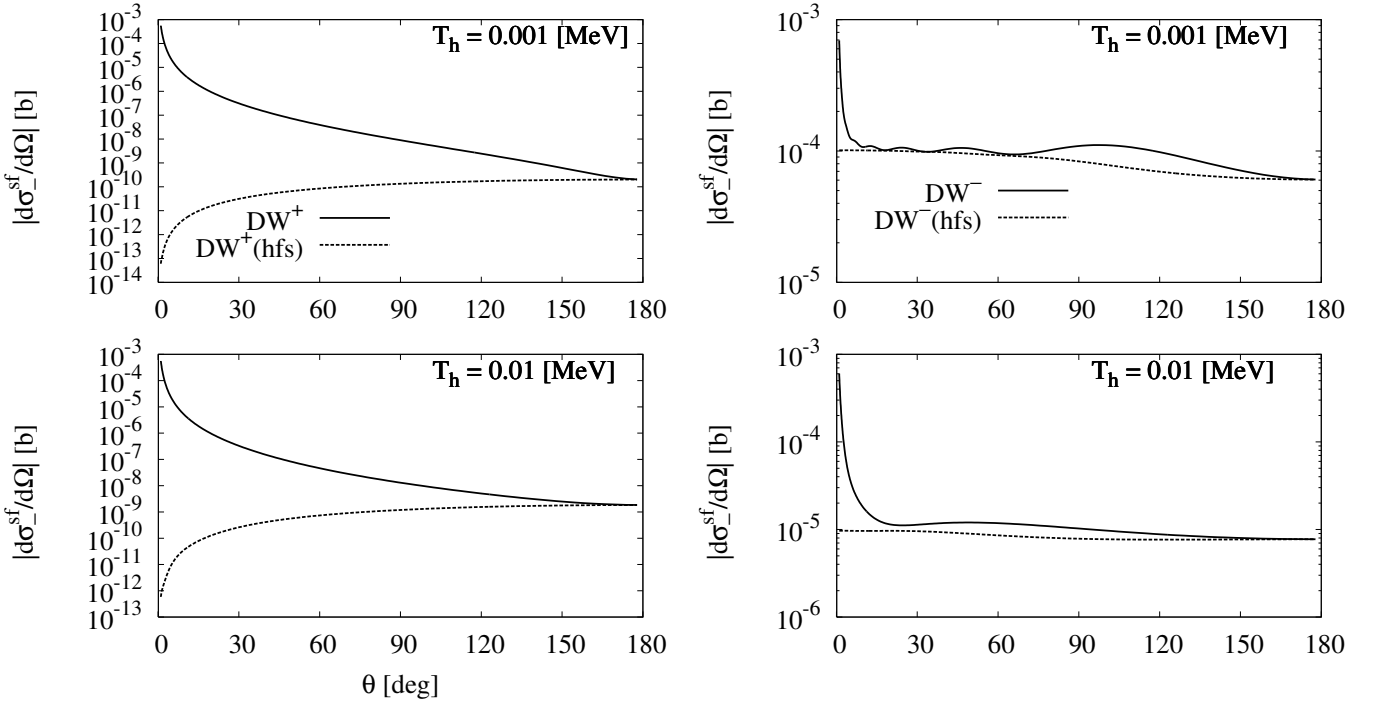


FIG. 10: Comparison of spin-flip cross section $d\sigma_{\pm}^{sf}/d\Omega$ for initial hadron polarization opposite to lepton polarization along the initial relative momentum with the hyperfine interaction alone (DW(hfs)) and with inclusion of the spin-orbit contribution (DW) for like charges (DW^+ , left panels) and opposite charges (DW^- , right panels) for the two lowest proton lab kinetic energies T_h .

and 3). Much more important is the leptonic spin-orbit contribution which, however, appears in the non-spin-flip cross section only (see eq. (111)) where it is buried completely by the Coulomb contribution S_C .

The results for the spin-flip cross section for parallel initial spin orientations of hadron and lepton is shown in Fig. 7 while the one for the opposite spin orientation in Fig. 8. One notes again the strong influence of Coulomb distortion. Furthermore, the leptonic spin-orbit interaction plays a relatively important role in the region of the minimum as can be seen in Figs. 9 and 10 where a comparison is exhibited with the case for which the spin-orbit interaction is switched off (curves labeled “(hfs)”). One readily notes a substantial increase when the spin-orbit part is included compared to the pure hyperfine case. Furthermore, at the lowest two energies the spin-orbit interaction induces oscillations, in particular in the forward direction. The difference of the two spin-flip cross sections determines the net hadron polarization in a storage ring of initially unpolarized hadrons scattered at polarized leptons.

The non-spin-flip cross section in eq. (111) is overwhelmingly dominated by the Coulomb contribution S_C . The small dependence on λ_l^i and λ_h leads to different scattering strengths for the hadron polarization parallel or antiparallel to the lepton polarization (see eq. (112)). The resulting lepton-hadron polarization transfer P_{z00z} is shown in Fig. 11. The dominance of the hyperfine amplitude is clearly seen.

C. The integrated structure functions and cross sections

Finally, I will present results for the integrated structure functions and spin-flip cross sections which are the relevant quantities for the polarization build-up in a storage ring. They are defined by the integration over the solid angle except for the small cone in the forward direction with $\theta < \theta_{min}$, where the minimal scattering angle is defined by the requirement that the impact parameter should not exceed a given value b

$$\theta_{min} = 2 \arctan(\eta_C/l), \quad (120)$$

with $l = bp$ as classical angular momentum. In the present work I have chosen $b = 10^{10}$. The choice of this value has been justified in ref. [3]. The dependence on this parameter is discussed below. Thus for any structure function or cross section $\mathcal{O}(\theta)$ I define

$$\langle \mathcal{O} \rangle = 2\pi \int_{\theta_{min}}^{\pi} d(\cos \theta) \mathcal{O}(\theta). \quad (121)$$

For the plane wave approximation, one finds easily the following expressions

$$\langle L_0^{l/h}(\theta) \rangle = -2\pi V (c_l^{LS})^2 \left(\ln(\sin(\theta_{min}/2)) + \frac{1}{2} \cos^2(\theta_{min}/2) \right), \quad (122)$$

$$\langle L_2^{l/h}(\theta) \rangle = -2\pi V c_l^{LS} c^{SS} \left(1 - \sin^2(\theta_{min}/2)(1 + \cos^2(\theta_{min}/2)) \right), \quad (123)$$

$$\langle S_0(\theta) \rangle = 8\pi V (c^{SS})^2, \quad (124)$$

$$\langle S_2^+(\theta) \rangle = 4\pi V \frac{c^{SS}}{p^2} \left(\ln(\sin(\theta_{min}/2)) - \frac{1}{2} \cos^2(\theta_{min}/2) \right), \quad (125)$$

$$\langle S_2^-(\theta) \rangle = -4\pi V (c^{SS})^2 \cos^2(\theta_{min}/2)(1 + \sin^2(\theta_{min}/2)), \quad (126)$$

$$\langle S_2(\theta) \rangle = -4\pi V (c^{SS})^2 (3 - \sin^4(\theta_{min}/2)). \quad (127)$$

Thus in plane wave all of the integrated structure functions except for $\langle S_2^+ \rangle$ are almost independent of T_h except for a very weak dependence via the minimal scattering angle. One should note the logarithmic divergence for $\theta_{min} \rightarrow 0$ in $\langle L_0^{l/h} \rangle$ and $\langle S_2^+ \rangle$. It corresponds to the logarithmic divergence in the angular momentum l of the partial wave expansion noted in ref. [4] which appears when integrating over the whole range of scattering angles.

The results are exhibited in Figs. 12 through 14 for the structure functions and in Fig. 15 for the spin-flip cross sections. The integrated structure functions show a strong increasing influence of Coulomb distortion with decreasing hadron kinetic energy T_h leading to large enhancements for opposite charges and strong suppression for like charges compared to the plane wave case. The only exception is $\langle S_2^+ \rangle$ for which Coulomb distortion results in a reduction for both cases, however much stronger for like charges. The reason for this feature is the strong oscillatory behavior in the angular distribution of $\langle S_2^+ \rangle$ at low T_h (see Fig. 5).

The integrated spin-flip cross section is given by

$$\langle \sigma_{\pm}^{sf} \rangle = 2\langle L_0^h \rangle - \langle S_2 \rangle + 2 \pm \left[\langle S_2^- \rangle + \langle L_2^h \rangle \right]. \quad (128)$$

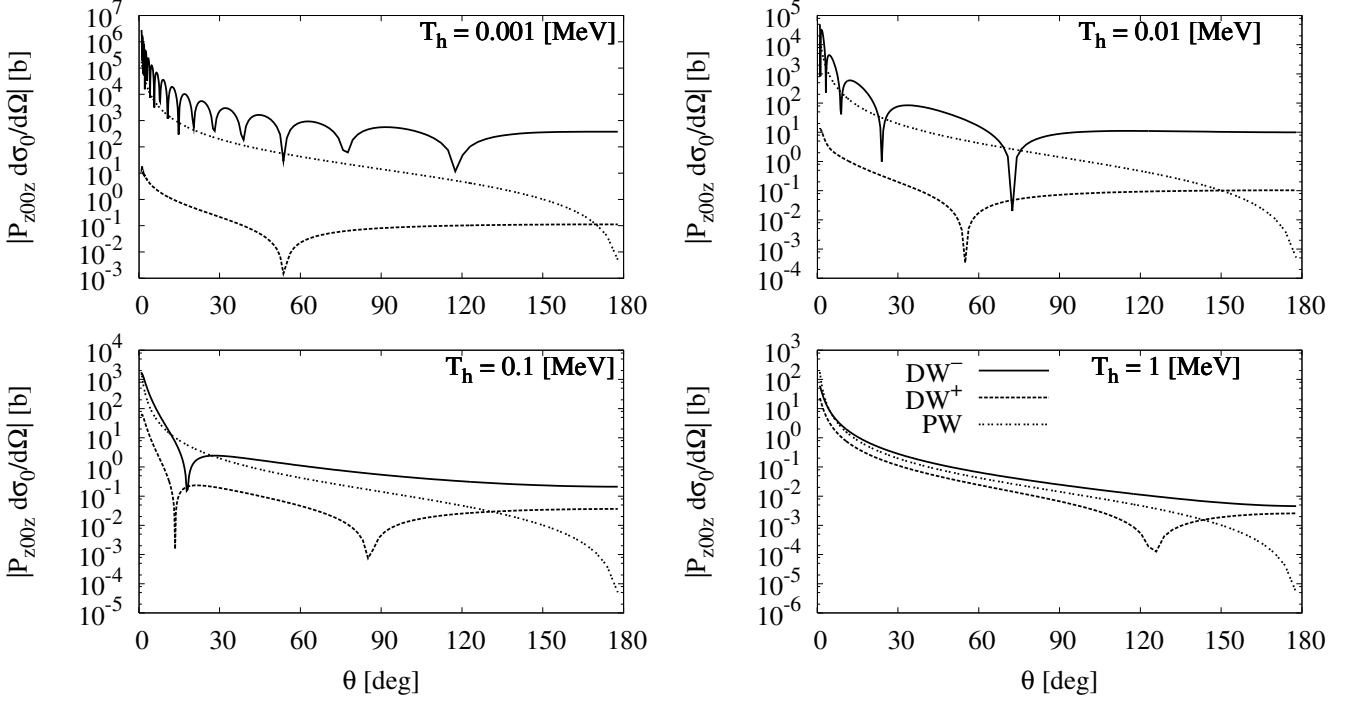


FIG. 11: Lepton-hadron polarization transfer cross section $P_{z00z}d\sigma_0/d\Omega$ with inclusion of spin-orbit contribution for like charges (DW^+) and opposite charges (DW^-) for several proton lab kinetic energies T_h .

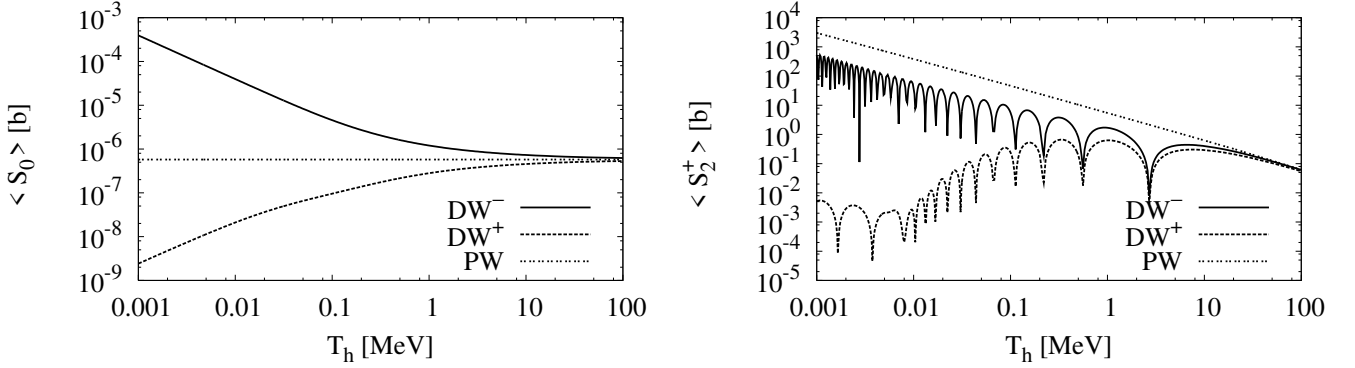


FIG. 12: The integrated structure functions $\langle S_0 \rangle$ (left panel) and $\langle S_2^+ \rangle$ (right panel) as function of the proton lab kinetic energy T_h for plane wave approximation (PW) and with Coulomb distortion for like charges (DW^+) and opposite charges (DW^-).

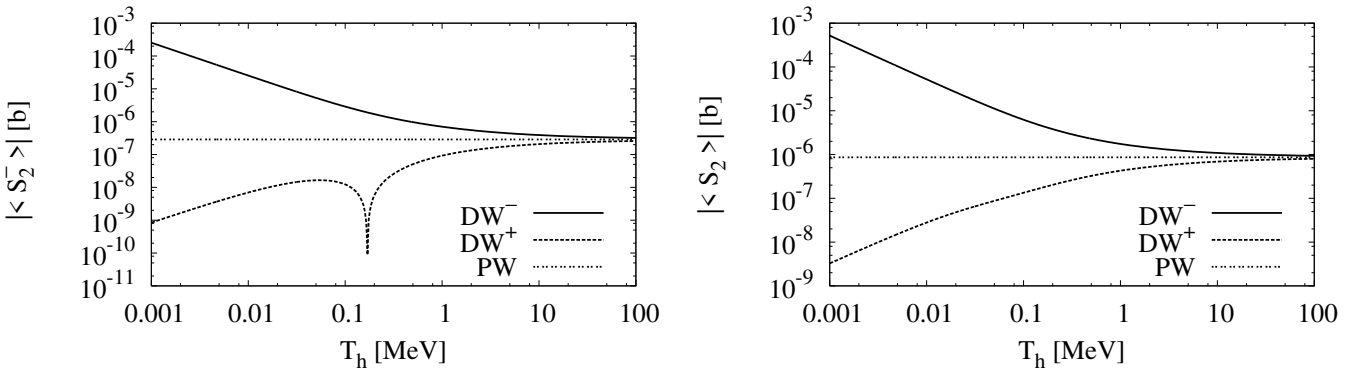


FIG. 13: The integrated structure functions $\langle S_2^- \rangle$ (left panel) and $\langle S_2 \rangle$ (right panel) as function of the proton lab kinetic energy T_h for plane wave approximation (PW) and with Coulomb distortion for like charges (DW^+) and opposite charges (DW^-).

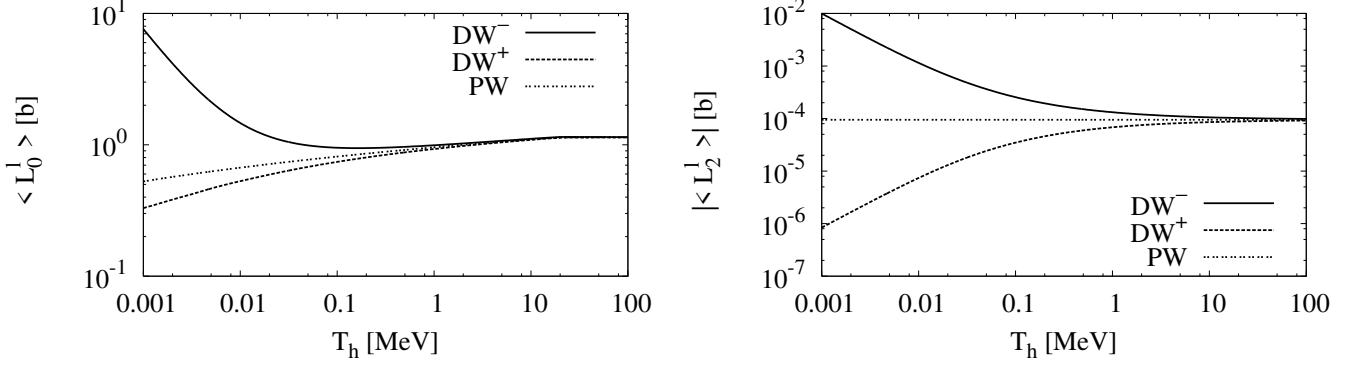


FIG. 14: The integrated structure functions $\langle L_0^l \rangle$ (left panel) and $|\langle L_2^l \rangle|$ (right panel) as function of the proton lab kinetic energy T_h for plane wave approximation (PW) and with Coulomb distortion for like charges (DW^+) and opposite charges (DW^-).

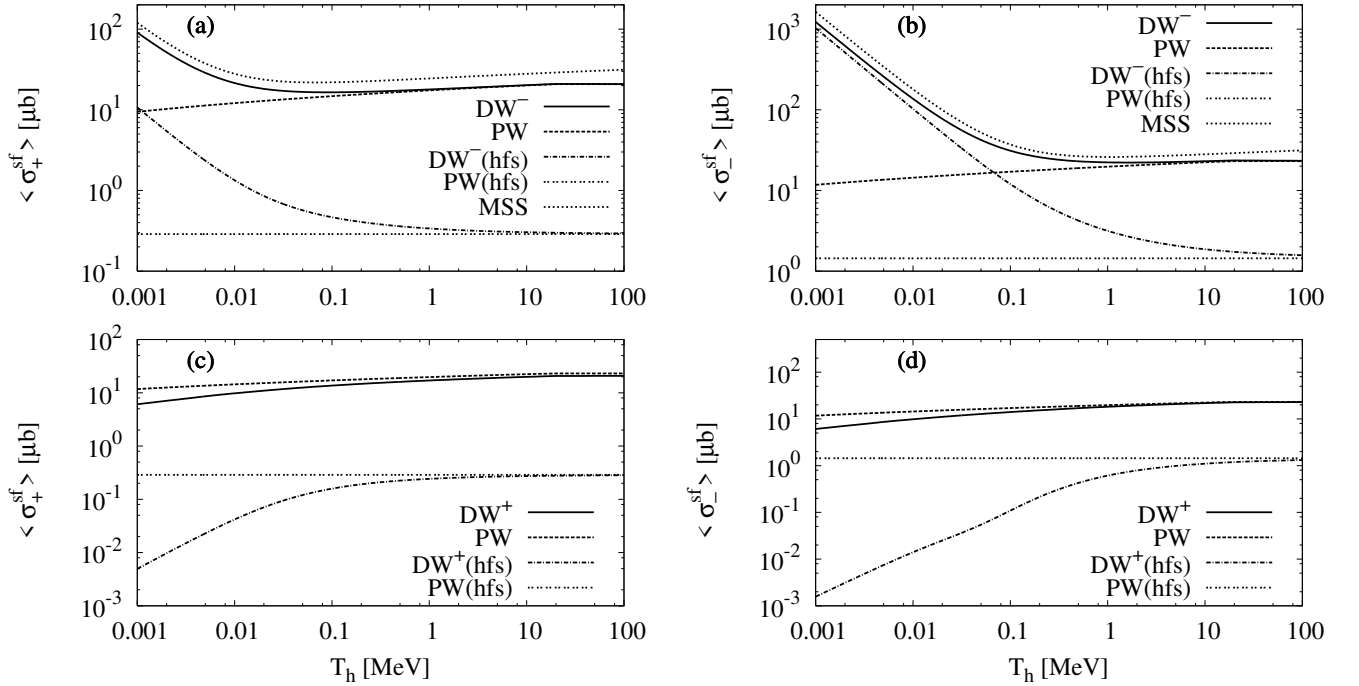


FIG. 15: The integrated spin-flip cross section $\langle \sigma_+^{sf} \rangle$ (left panels) and $\langle \sigma_-^{sf} \rangle$ (right panels) as function of the proton lab kinetic energy T_h for plane wave approximation (PW) and with Coulomb distortion for like charges (DW^+ , lower panels) and opposite charges (DW^- , upper panels). Curves labeled “hfs” include the hyperfine amplitude only, and in the upper panels the curves labeled “MSS” represent the results of ref. [4].

The corresponding integrated spin flip cross section of Milstein et al. [4] reads according to their eq. (21)

$$\langle \sigma_{\pm}^{sf} \rangle_{MSS} = \pi \left(\frac{\alpha \mu_p}{M_p} \right)^2 \left[(2\pi\eta_C)^2 \left(\frac{11}{6} - \ln 2 \right) + \ln(l_{max}/\eta_C)^2 \mp (2\pi\eta_C)^2 \right]. \quad (129)$$

The appearing logarithmic divergence in the angular momentum l is regularized by choosing a finite l_{max} determined by the classical relation $l_{max} = bp$ which corresponds to the choice of a minimum scattering angle in the present work. The integrated strength of the spin-flip cross sections in Fig. 15 shows as expected with decreasing T_h a growing strong influence of Coulomb effects via the hyperfine and hadronic spin-orbit interactions. The latter is only important in the spin-independent part of the spin-flip cross section while its influence in the spin-dependent part is negligible. The results of Milstein et al. [4], shown in the upper panels of Fig. 15 for opposite charges, are comparable to our results but display a slight overestimation which is probably due to different approximations in [4]. The dependence of the integrated spin-flip cross section for opposite charges on the

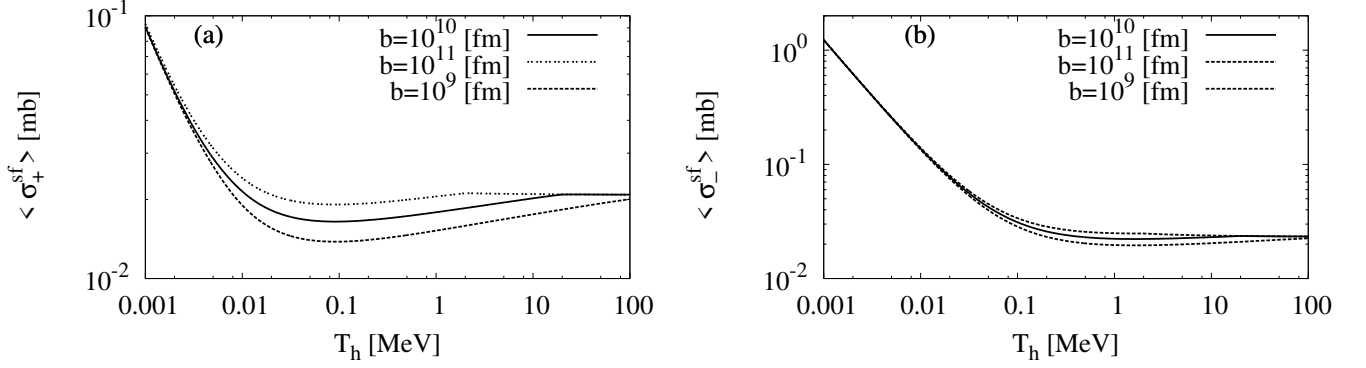


FIG. 16: Dependence of the integrated spin-flip cross sections for opposite charges on the regularization parameter b .

regularization parameter b is exhibited in Fig. 16 for $b = 10^9, 10^{10}$ and 10^{11} fm. It appears to be quite weak.

The relevant quantity for a polarization build-up in a storage ring is the ratio of the spin-independent part over the spin-dependent part

$$R^{sf} = 2 \frac{\langle S_2^- \rangle + \langle L_2^h \rangle}{2\langle L_0^h \rangle - \langle S_2 \rangle}, \quad (130)$$

which is shown in Fig. 17. One readily notes the reduction of this ratio by the hadronic spin-orbit interaction, in particular quite strong at higher energies but only about 12 % at the lowest energy. This fact clearly shows the importance of the hadronic spin-orbit interaction besides the hyperfine contribution.

Finally, I show for completeness in Fig. 18 the integrated polarization transfer cross section $\langle P_{z00z} \sigma_0 \rangle$. It is dominated by the hyperfine interaction whereas the spin-orbit contribution is negligible.

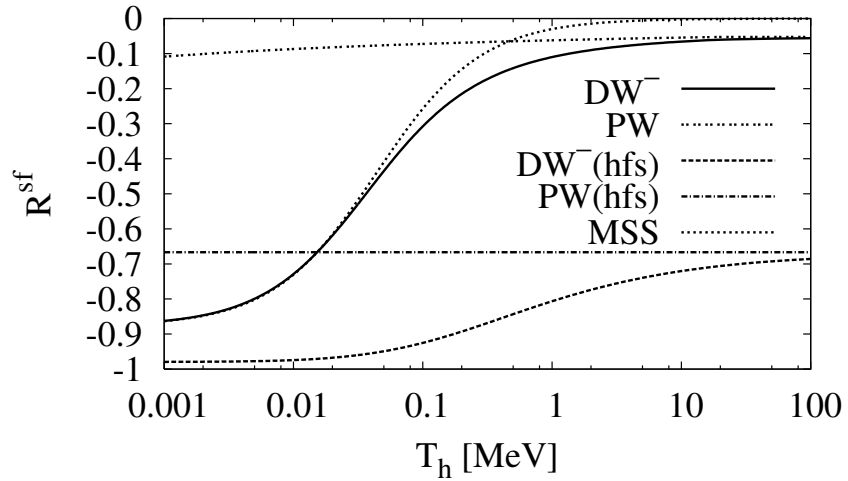


FIG. 17: Ratio of the spin dependent part of the spin-flip cross section over its spin-independent part as function of the proton lab kinetic energy T_h for plane wave approximation (PW) and with Coulomb distortion for opposite charges (DW^-): present calculation and the result of ref. [4] (MSS). For the curves labeled (hfs) only the hyperfine amplitude is included.

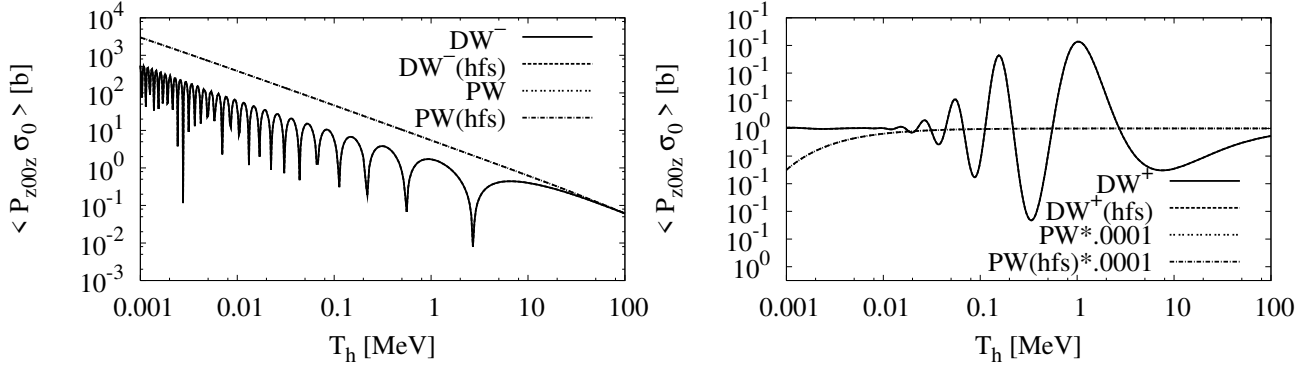


FIG. 18: The integrated polarization transfer cross section $\langle P_{z00z} \sigma_0 \rangle$ as function of the proton lab kinetic energy T_h for plane wave approximation (PW) and with Coulomb distortion for like charges (DW⁺, right panel) and opposite charges (DW⁻, left panel). For the curves labeled (hfs) only the hyperfine amplitude is included.

V. CONCLUSIONS

Formal expressions for polarization observables in electromagnetic hadron-lepton scattering have been derived within a non-relativistic framework including the central Coulomb force as well as the lepton and hadron spin-orbit and hyperfine interactions. The latter have been treated in a distorted wave approximation. Special emphasis has been laid on the triple polarization cross section with polarizations of the initial hadron and lepton and of the final hadron along the incoming hadron momentum. The structure functions which determine the differential triple polarization cross section have been evaluated in plane and distorted wave approximations for hadron lab kinetic energies between 1 keV and 100 MeV.

For the evaluation of the Coulomb distortion two different methods have been employed: (i) an integral representation of the nonrelativistic Coulomb scattering wave function and (ii) a partial wave expansion. These two independent methods have served as a mutual check for the numerical accuracy of the results.

As expected, the distortion effects are very important at low energies in the small polarization observables, which are driven by the spin-orbit and hyperfine interactions, leading to sizeable enhancements for opposite charges and suppressions for like charges according to the Coulomb attraction resp. repulsion. This is shown in detail for the structure functions of the triple polarization cross section and for the special case of the spin-flip differential cross section.

The leptonic spin-orbit interactions plays a minor role in the non-spin-flip cross section in its spin-dependent part, which, however, as a whole is by many orders of magnitude smaller than the spin-independent part, dominated by the Coulomb term S_C . The influence of the spin-orbit and hyperfine interactions on the unpolarized cross section is almost negligible in the whole range of energies studied here.

With respect to the integrated spin-flip cross sections our previous work has been extended by the inclusion of the hadronic spin-orbit interaction which shows a non-negligible effect in the spin-independent part changing sizeably the ratio of the integrated strength of its spin-dependent over the spin-independent part.

Acknowledgment

I would like to thank Thomas Walcher for his continued interest in this work and for many useful discussions. This work has been supported by the SFB 443 of the Deutsche Forschungsgemeinschaft.

Appendix: Evaluation of hyperfine and spin-orbit interaction

For the evaluation of the Coulomb distortion of the amplitude b of the spin-orbit interaction in DWBA as given in eq. (36) and the tensor amplitudes $d^{[2]}$ of the hyperfine interaction in eq. (39) two different method have been applied: (i) An integral representation and (ii) a partial wave expansion of the Coulomb wave function. For convenience I set in this appendix $\eta = \eta_C$.

1. Integral representation

In [1] a detailed description of this method for the evaluation of $d^{[2]}$ has been given. Therefore, I will only summarize the result. The method is based on an integral representation of the confluent hypergeometric function as proposed in [7]

$${}_1F_1(-i\eta, 1; ix) = Q(\eta) \int_0^1 dt f(t, \eta) \left(1 + t \frac{\partial}{\partial t}\right) e^{ix(1-t)}, \quad (\text{A.1})$$

with

$$Q(\eta) = \frac{\sinh \pi \eta}{\pi \eta}, \quad \text{and } f(t, \eta) = e^{i\eta \ln \frac{t}{1-t}}. \quad (\text{A.2})$$

With the help of this representation, the hyperfine tensor $d_{ij}^{[2]}$ and the spin orbit vector \mathbf{b} are expressed as two-dimensional integrals, as described below.

Hyperfine interaction

For the hyperfine tensor one finds

$$d_{ij}^{[2]}(\eta, \theta) = c^{SS} N(\eta) \left[\tilde{d}_{ij}^{[2]}(1, \eta, \theta) + i\eta \int_0^1 \frac{dt}{1-t} e^{-i\eta \ln(1-t)} \left(\tilde{d}_{ij}^{[2]}(1, \eta, \theta) - e^{i\eta \ln t} \tilde{d}_{ij}^{[2]}(t, \eta, \theta) \right) \right], \quad (\text{A.3})$$

where

$$N(\eta) = e^{-\pi \eta} \frac{\sinh(\pi \eta)}{\pi \eta} \quad (\text{A.4})$$

is a normalization factor and

$$\begin{aligned} \tilde{d}_{ij}^{[2]}(t, \eta, \theta) &= A_{ij}(t, 1, \eta, \theta) I_{SS}(c(t, 1)) \\ &+ i\eta \int_0^1 \frac{dt'}{1-t'} e^{-i\eta \ln(1-t')} \left(A_{ij}(t, 1) I(c(t, 1)) - e^{i\eta \ln t'} A_{ij}(t, t') I_{SS}(c(t, t')) \right). \end{aligned} \quad (\text{A.5})$$

Here I have introduced the tensor

$$A_{ij}(t, t') = 3\hat{a}_i(t, t') \hat{a}_j(t, t') - \delta_{ij}, \quad (\text{A.6})$$

with

$$\hat{a}(t, t') = \frac{\mathbf{p}t - \mathbf{p}'t'}{pg(t, t')}, \quad (\text{A.7})$$

and

$$g(t, t') = [t^2 + t'^2 - 2tt' \cos \theta]^{1/2}. \quad (\text{A.8})$$

Furthermore, $I_{SS}(c)$ denotes the integral

$$\begin{aligned} I_{SS}(c) &= \int_0^\infty \frac{dx}{x} e^{icx} j_2(x) \\ &= \frac{1}{3} - \frac{1}{2} c^2 - \frac{1}{4} c(1-c^2) \left(\ln \left| \frac{c+1}{c-1} \right| - i\pi \Theta(1-c) \right), \end{aligned} \quad (\text{A.9})$$

with $\Theta(x)$ as the Heaviside step function and

$$c(t, t') = \frac{2-t-t'}{g(t, t')}. \quad (\text{A.10})$$

One should note that $d_{ij}^{[2]}$ and $\tilde{d}_{ij}^{[2]}(t)$ are functions in θ and ϕ , the scattering angles in the c.m. frame. However, as mentioned above, it suffices to choose $\phi = 0$.

The remaining integrations over t and t' in eqs. (A.3) and (A.5) are evaluated numerically. Details are presented in [1]. However, I would like to mention that in contrast to eq. (A.36) of ref. [1], I found it more advantageous to use for the numerical evaluation a transformation of the integration variable $y = -\ln(1-t)$ resulting in

$$\int_0^1 \frac{dt}{1-t} e^{-i\eta \ln(1-t)} (g(1) - g(t)) = \int_0^\infty dy e^{i\eta y} (g(1) - g(1 - e^{-y})). \quad (\text{A.11})$$

As mentioned in the appendix of ref. [1], it is useful to separate the contributions of the real and imaginary part of the radial integral I_{SS} for $\eta > 0$ according to

$$d_{ij}^{[2]}(\eta, \theta) = N(\eta) \left(\mathcal{R}_{ij}^{SS}(\eta, \theta) + \mathcal{I}_{ij}^{SS}(\eta, \theta) \right), \quad (\text{A.12})$$

where $\mathcal{R}/\mathcal{I}_{ij}^{SS}$ - from now on called reduced amplitudes - refer to the contributions of ReI_{SS} and ImI_{SS} , respectively (see eq. (A.9)), to $\tilde{d}_{ij}^{[2]}(t, \eta, \theta)$ in eq. (A.5). With respect to the symmetry under sign change of η , one finds easily the properties

$$\mathcal{R}_{ij}^{SS}(\theta, -\eta) = (\mathcal{R}_{ij}^{SS}(\eta, \theta))^*, \quad (\text{A.13})$$

$$\mathcal{I}_{ij}^{SS}(\theta, -\eta) = -(\mathcal{I}_{ij}^{SS}(\eta, \theta))^*, \quad (\text{A.14})$$

from which follows

$$d_{ij}^{[2]}(\theta, -\eta) = N(-\eta) \left(\mathcal{R}_{ij}^{SS}(\eta, \theta) - \mathcal{I}_{ij}^{SS}(\eta, \theta) \right)^*, \quad (\text{A.15})$$

Thus it suffices to evaluate the reduced amplitudes $\mathcal{R}/\mathcal{I}_{ij}^{SS}$ for $\eta > 0$ from which one can determine $d_{ij}^{[2]}(\theta, \pm\eta)$ applying eqs. (A.12) and (A.15). On the other hand, given $d_{ij}^{[2]}(\theta, \pm\eta)$ the reduced amplitudes are obtained from

$$\mathcal{R}_{ij}^{SS}(\eta, \theta) = \frac{1}{2} \left(\frac{d_{ij}^{[2]}(\eta, \theta)}{N(\eta)} + \frac{d_{ij}^{[2]}(\theta, -\eta)^*}{N(-\eta)} \right) = \frac{1}{2N(\eta)} \left(d_{ij}^{[2]}(\eta, \theta) + e^{-2\pi\eta} d_{ij}^{[2]}(\theta, -\eta)^* \right), \quad (\text{A.16})$$

$$\mathcal{I}_{ij}^{SS}(\eta, \theta) = \frac{1}{2} \left(\frac{d_{ij}^{[2]}(\eta, \theta)}{N(\eta)} - \frac{d_{ij}^{[2]}(\theta, -\eta)^*}{N(-\eta)} \right) = \frac{1}{2N(\eta)} \left(d_{ij}^{[2]}(\eta, \theta) - e^{-2\pi\eta} d_{ij}^{[2]}(\theta, -\eta)^* \right). \quad (\text{A.17})$$

These relations are useful for the comparison with the partial wave approach. In addition, they show that for large positive η the second terms in eqs. (A.16) and (A.17) are strongly suppressed by the factor $e^{-2\pi\eta}$. Consequently, one finds that $\mathcal{R}_{ij}^{SS}(\eta, \theta) \approx \mathcal{I}_{ij}^{SS}(\eta, \theta)$ for positive $\eta \gg 1$. This feature poses a serious problem for the numerical evaluation of $d_{ij}^{[2]}(\theta, -\eta)$ for $\eta \gg 1$ because it is proportional to the difference of the reduced amplitudes and multiplied with a huge number ($N(-\eta)$) according to eq. (A.15). Thus with increasing absolute value of η more and more significant digits are lost in the difference for negative η . An example is presented later.

a. Spin-orbit interaction

Following the analogous steps for the spin-orbit interaction, one finds

$$\mathbf{b}(\theta, \phi) = i b_0(\eta, \theta) \frac{\mathbf{p}' \times \mathbf{p}}{|\mathbf{p}' \times \mathbf{p}|} \quad (\text{A.18})$$

where

$$b_0(\eta, \theta) = c^{LS} \sin \theta N(\eta) \left[\tilde{b}_0(\theta, 1, \eta) + i\eta \int_0^1 \frac{dt}{1-t} e^{-i\eta \ln(1-t)} \left(\tilde{b}_0(\theta, 1, \eta) - e^{i\eta \ln t} \tilde{b}_0(\theta, t, \eta) \right) \right], \quad (\text{A.19})$$

$$\tilde{b}_0(\theta, t, \eta) = \frac{I_{LS}(c(t, 1))}{g(t, 1)^2} + i\eta \int_0^1 \frac{dt'}{1-t'} e^{-i\eta \ln(1-t')} \left(\frac{I_{LS}(c(t, 1))}{g(t, 1)^2} - e^{i\eta \ln t'} \frac{t' I_{LS}(c(t, t'))}{g(t, t')^2} \right), \quad (\text{A.20})$$

with $g(t, t')$ in eq. (A.8) and the radial integral

$$I_{LS}(c) = \int_0^\infty \frac{dx}{x} e^{icx} j_1(x) = 1 - \frac{c}{2} \ln \left| \frac{c+1}{c-1} \right| + i \frac{\pi c}{2} \Theta(1-c). \quad (\text{A.21})$$

The numerical evaluation is analogous to the one for the hyperfine interaction. For $\eta = 0$ one finds $b_0(0, \theta) = e^{LS} \sin \theta / (4 \sin^2 \theta / 2)$ and thus

$$\mathbf{b}^{PW}(\theta, \phi) = \frac{i}{2} \cot(\theta/2) e^{LS} \frac{\mathbf{p}' \times \mathbf{p}}{|\mathbf{p}' \times \mathbf{p}|} \quad (\text{A.22})$$

in agreement with eq. (23).

Also in this case I introduce reduced amplitudes by separating the contributions of the real and imaginary parts of the radial integral I_{LS} according to

$$b_0(\eta, \theta) = N(\eta) \left(\mathcal{R}^{LS}(\eta, \theta) + \mathcal{I}^{LS}(\eta, \theta) \right), \quad (\text{A.23})$$

such that

$$b_0(\theta, -\eta) = N(-\eta) \left(\mathcal{R}^{LS}(\eta, \theta) - \mathcal{I}^{LS}(\eta, \theta) \right)^*, \quad (\text{A.24})$$

and

$$\mathcal{R}^{LS}(\eta, \theta) = \frac{1}{2N(\eta)} \left(b_0(\eta, \theta) + e^{-2\pi\eta} b_0(\theta, -\eta)^* \right), \quad (\text{A.25})$$

$$\mathcal{I}^{LS}(\eta, \theta) = \frac{1}{2N(\eta)} \left(b_0(\eta, \theta) - e^{-2\pi\eta} b_0(\theta, -\eta)^* \right). \quad (\text{A.26})$$

Again numerical problems arise for negative η with $|\eta| \gg 1$ as for the hyperfine interaction outlined above.

2. Partial wave expansion

The expansion of the Coulomb wave function into partial waves reads

$$\psi_{\mathbf{p}}^{(+)}(\mathbf{r}) = \frac{4\pi}{pr} \sum_{l,m} i^l e^{i\bar{\sigma}_l} F_l(\eta, pr) Y_{lm}^*(\hat{r}) Y_{lm}(\hat{p}) \quad (\text{A.27})$$

where the radial function F_l is given in terms of the confluent hypergeometric function ${}_1F_1(a, b, z)$

$$F_l(\eta, \rho) = C_l(\eta) e^{i\rho} \rho^{l+1} {}_1F_1(l+1 + i\eta, 2l+2, -2i\rho), \quad (\text{A.28})$$

and constants depending on the Sommerfeld parameter η

$$\begin{aligned} C_l(\eta) &= \frac{2^l}{(2l+1)!} e^{-\frac{\pi}{2}\eta} |\Gamma(l+1 + i\eta)| \\ &= \frac{C_0(\eta)}{(2l+1)!!} D_l(\eta^2), \end{aligned} \quad (\text{A.29})$$

$$C_0(\eta) = e^{-\frac{\pi}{2}\eta} |\Gamma(1 + i\eta)| = e^{-\frac{\pi}{2}\eta} \sqrt{\frac{\pi\eta}{\sinh(\pi\eta)}}, \quad (\text{A.30})$$

$$D_l(\eta^2) = \prod_{n=1}^l \sqrt{1 + \left(\frac{\eta}{n}\right)^2}. \quad (\text{A.31})$$

In the above expression, I have separated as in eq. (31) the $l = 0$ phase $\sigma_0 = \sigma_C$ for convenience, coinciding with the Coulomb phase σ_C given in eq. (33). The remaining partial wave phase is given by

$$\bar{\sigma}_l = \sigma_l - \sigma_0, \quad (\text{A.32})$$

where for $l > 0$

$$e^{i\bar{\sigma}_l} = \frac{l + i\eta}{|l + i\eta|} \cdots \frac{1 + i\eta}{|1 + i\eta|}. \quad (\text{A.33})$$

Evaluation of the various contributions to the scattering matrix as listed in eqs. (36) and (39) leads to the following expressions which are still operators in spin space

$$\mathbf{b}_{l/h}^{DW} \cdot \boldsymbol{\sigma}_{l/h} = \sum_{l=1}^{\infty} G_{LS_{l/h}}^l \boldsymbol{\Omega}_{ll}(\hat{p}', \hat{p}) \cdot \boldsymbol{\sigma}_{l/h}, \quad (\text{A.34})$$

$$\sum_{ij} \sigma_{l,i} d_{ij}^{[2]} \sigma_{h,j} = \sum_{l'=0}^{\infty} \sum_{l=0}^{\infty} G_{SS,2}^{l'l} \left[\Sigma^{[2]}(\boldsymbol{\sigma}_l, \boldsymbol{\sigma}_h) \times \Omega_{l'l}^{[2]} \right]^{[0]}(\hat{p}', \hat{p}), \quad (\text{A.35})$$

where I have introduced for convenience in the notation of Fano and Racah [12] for irreducible spherical tensors

$$\Omega_{l'l}^{[K]}(\hat{p}', \hat{p}) = \left[Y^{[l']}(\hat{p}') \times Y^{[l]}(\hat{p}) \right]^{[K]}, \quad (\text{A.36})$$

$$\Sigma^{[2]}(\boldsymbol{\sigma}_l, \boldsymbol{\sigma}_h) = \left[\sigma_l^{[1]} \times \sigma_h^{[1]} \right]^{[2]}. \quad (\text{A.37})$$

The coefficients are given in terms of the radial matrix elements $R_{l'l}$ (note the meaning of the ‘‘hat symbol’’: $\hat{l} = \sqrt{2l+1}$)

$$G_{LS_{l/h}}^l(\eta) = (-)^{l+1} \frac{4\pi}{\sqrt{3}} c_{l/h}^{LS} \hat{l} \sqrt{l(l+1)} e^{2i\bar{\sigma}_l} R_{ll}. \quad (\text{A.38})$$

$$G_{SS,2}^{l'l}(\eta) = i^{l-l'} 16 \pi \sqrt{6} c^{SS} \hat{l} \hat{l}' e^{i(\bar{\sigma}_{l'} + \bar{\sigma}_l)} \begin{pmatrix} l' & l & 2 \\ 0 & 0 & 0 \end{pmatrix} R_{l'l}. \quad (\text{A.39})$$

with

$$R_{l'l} = \frac{4}{p^2} \int_0^{\infty} \frac{dr}{r^3} F_{l'}(\eta, pr) F_l(\eta, pr) = 4 \int_0^{\infty} \frac{d\rho}{\rho^3} F_{l'}(\eta, \rho) F_l(\eta, \rho). \quad (\text{A.40})$$

Besides the radial integral R_{ll} , only $R_{l'l} = R_{l'l'}$ for $|l-l'| = 2$ are needed in view of the selection rule of the 3j-symbol in eq. (A.39). This radial integral is well known in Coulomb excitation (see e.g. [13]). The explicit form of the radial integral is also given in [4]. For $l' = l$ and $l > 0$ one has

$$R_{ll} = \frac{2}{l(l+1)} \left(1 + \frac{f_l(\eta)}{2l+1} \right) \quad (\text{A.41})$$

with

$$f_l(\eta) = e^{-\pi\eta} \frac{\pi\eta}{\sinh(\pi\eta)} - 1 - 2\eta^2 \sum_{k=1}^l \frac{1}{k^2 + \eta^2}. \quad (\text{A.42})$$

One should note that f_l vanishes for $\eta = 0$. For $|l'-l| = 2$ one has

$$R_{l,l+2} = \frac{2}{3|l+1+i\eta||l+2+i\eta|}. \quad (\text{A.43})$$

a. The hyperfine contribution

The tensor amplitude $d_{ij}^{[2]}$ of the hyperfine interaction is obtained by separating the spin dependence in eq. (A.35). This means, one has to evaluate

$$\begin{aligned} d_{ij}^{[2]} &= \frac{\partial^2}{\partial \sigma_{l,i} \partial \sigma_{h,j}} \sum_{ij} \sigma_{l,i} d_{ij}^{[2]} \sigma_{h,j} \\ &= \sum_{l'=0}^{\infty} \sum_{l=0}^{\infty} G_{SS,2}^{l'l} \frac{\partial^2}{\partial \sigma_{l,i} \partial \sigma_{h,j}} \left[\Sigma^{[2]}(\boldsymbol{\sigma}_l, \boldsymbol{\sigma}_h) \times \Omega_{l'l}^{[2]} \right]^{[0]}(\hat{p}', \hat{p}). \end{aligned} \quad (\text{A.44})$$

It suffices to consider $d_{ij}^{[2],0}$ for the special case, for which the scattering plane coincides with the x - z -plane, i.e. $\hat{p}' = (\sin \theta, 0, \cos \theta)$. First one notes that then

$$\Omega_{l'l,m}^{[2]}(\hat{p}', \hat{p}) = \frac{\sqrt{5}}{4\pi} (-)^{l+1} \hat{l} \hat{l}' \sum_m \sqrt{\frac{(l-m)!}{(l+m)!}} \begin{pmatrix} l' & l & 2 \\ m & 0 & -m \end{pmatrix} P_l^m(\cos \theta), \quad (\text{A.45})$$

where P_l^m denotes the associated Legendre function, and thus

$$\frac{\partial^2}{\partial \sigma_{l,i} \partial \sigma_{h,j}} \left[\Sigma^{[2]}(\boldsymbol{\sigma}_l, \boldsymbol{\sigma}_h) \times \Omega_{l'}^{[2]} \right]^{[0]} = \frac{\sqrt{5}}{4\pi} (-)^{l+l'} \hat{l}' \hat{l} \sqrt{\frac{(l-m)!}{(l+m)!}} \begin{pmatrix} l' & l & 2 \\ m & 0 & -m \end{pmatrix} P_l^m(\cos \theta) \sigma_{ij}^m, \quad (\text{A.46})$$

where

$$\sigma_{ij}^m = \frac{\partial^2}{\partial \sigma_{l,i} \partial \sigma_{h,j}} \Sigma_m^{[2]}(\boldsymbol{\sigma}_l, \boldsymbol{\sigma}_h). \quad (\text{A.47})$$

With these expressions one finds for the tensor part of the hyperfine contribution

$$d_{ij}^{[2],0} = \frac{\sqrt{3}}{2\sqrt{2}} c^{SS} \sum_l^\infty \left[S_l^0 P_l(\cos \theta) \sigma_{ij}^0 + S_l^1 \sqrt{\frac{(l-1)!}{(l+1)!}} P_l^1(\cos \theta) (\sigma_{ij}^1 - \sigma_{ij}^{-1}) + S_l^2 \sqrt{\frac{(l-2)!}{(l+2)!}} P_l^2(\cos \theta) (\sigma_{ij}^2 + \sigma_{ij}^{-2}) \right], \quad (\text{A.48})$$

where for $m = 0, 1, 2$

$$S_l^m = (-i)^{l-\hat{l}} e^{i\hat{\sigma}_l} \sum_{k=|l-2|}^{l+2} i^k \hat{k}^2 e^{i\hat{\sigma}_k} \begin{pmatrix} l & k & 2 \\ 0 & 0 & 0 \end{pmatrix} \begin{pmatrix} l & k & 2 \\ -m & 0 & m \end{pmatrix} R_{lk}. \quad (\text{A.49})$$

Explicitly, with

$$\sigma_{11/22}^m = -\frac{\delta_{m0}}{\sqrt{6}} \pm \frac{\delta_{|m|2}}{2}, \quad \sigma_{33}^m = \delta_{m0} \sqrt{\frac{2}{3}}, \quad \sigma_{12}^m = i \frac{m}{2} \delta_{|m|2}, \quad \sigma_{13}^m = -\frac{m}{2} \delta_{|m|1}, \quad \sigma_{23}^m = -\frac{i}{2} \delta_{|m|1}, \quad (\text{A.50})$$

one obtains for the nonvanishing components

$$d_{33}^{[2],0} = c^{SS} \sum_{l=0}^\infty S_l^{33} P_l(\cos \theta), \quad (\text{A.51})$$

$$d_{11/22}^{[2],0} = \pm c^{SS} \sum_{l=2}^\infty S_l^{11} P_l^2(\cos \theta) - \frac{1}{2} d_{33}^{[2],0}, \quad (\text{A.52})$$

$$d_{13}^{[2],0} = c^{SS} \sum_{l=1}^\infty S_l^{13} P_l^1(\cos \theta), \quad (\text{A.53})$$

where I have introduced for convenience

$$S_l^{33} = \frac{1}{2} S_l^0, \quad S_l^{11} = \frac{1}{2} \sqrt{\frac{3(l-2)!}{2(l+2)!}} S_l^2, \quad S_l^{13} = -\frac{1}{2} \sqrt{\frac{3(l-1)!}{2(l+1)!}} S_l^1. \quad (\text{A.54})$$

It is useful to separate the η -independent contributions, constituting the plane wave approximation. One finds explicitly the following detailed expressions

$$d_{33}^{[2],0}(\eta) = c^{SS} \left(\sin^2(\theta/2) - \frac{1}{3} + \sum_{l=0}^\infty \tilde{S}_l^{33}(\eta) P_l(\cos \theta) \right), \quad (\text{A.55})$$

$$d_{11/22}^{[2],0}(\eta) = \pm c^{SS} \left(\frac{1}{2} \cos^2(\theta/2) + \sum_{l=2}^\infty \tilde{S}_l^{11}(\eta) P_l^2(\cos \theta) \right) - \frac{1}{2} d_{33}^{[2],0}, \quad (\text{A.56})$$

$$d_{13}^{[2],0}(\eta) = c^{SS} \left(-\frac{1}{2} \sin(\theta) + \sum_{l=1}^\infty \tilde{S}_l^{13}(\eta) P_l^1(\cos \theta) \right), \quad (\text{A.57})$$

where the coefficients $\tilde{S}_l^{ij}(\eta)$ vanish for $\eta = 0$. In detail one finds for $i = j = 3$ and $l = 0, 1$

$$\tilde{S}_0^{33}(\eta) = \frac{i\eta}{3} \frac{3 - i\eta}{(1 - i\eta)(2 - i\eta)}, \quad (\text{A.58})$$

$$\tilde{S}_1^{33}(\eta) = -\frac{3}{5} \left[\frac{1 + i\eta}{1 - i\eta} \frac{f_1(\eta)}{3} - \frac{i\eta(5 - i\eta)}{6(2 - i\eta)(3 - i\eta)} - \frac{2i\eta}{1 - i\eta} \left(1 - \frac{1}{(2 - i\eta)(3 - i\eta)} \right) \right], \quad (\text{A.59})$$

and for $l > 1$

$$\tilde{S}_l^{33}(\eta) = -e^{2i\bar{\sigma}_l} \left[\frac{i\eta}{2} (b_l(\eta) - b_{l+2}(\eta)^*) + \frac{f_l(\eta)}{(2l-1)(2l+3)} \right]. \quad (\text{A.60})$$

Here I have introduced for convenience

$$b_l(\eta) = \frac{2l-1+i\eta}{(2l-1)(l-1)l(l-1+i\eta)(l+i\eta)}. \quad (\text{A.61})$$

One should note that the coefficients \tilde{S}_l^{33} behave as $1/l^2$ for $l \rightarrow \infty$.

For $i = j = 1$ one obtains (note $l > 1$)

$$\tilde{S}_l^{11}(\eta) = \frac{(2l+1)(1-e^{2i\bar{\sigma}_l})}{2(l-1)l(l+1)(l+2)} + e^{2i\bar{\sigma}_l} \left(\frac{i\eta}{4} (b_l(\eta) - b_{l+2}(\eta)^*) - \frac{3f_l(\eta)}{2l(l+1)(2l-1)(2l+3)} \right), \quad (\text{A.62})$$

The coefficient \tilde{S}_l^{11} behaves as l^{-3} for $l \rightarrow \infty$.

Finally, for \tilde{S}_l^{13} one obtains for $l = 1$

$$\tilde{S}_1^{13}(\eta) = \frac{3}{20} \left[\frac{1+i\eta}{1-i\eta} f_1(\eta) + \frac{5}{3} i\eta b_3(\eta)^* + \frac{2i\eta}{1-i\eta} \left(3 + \frac{2}{(2-i\eta)(3-i\eta)} \right) \right] \quad (\text{A.63})$$

and for $l > 1$

$$\tilde{S}_l^{13}(\eta) = \frac{1}{2} e^{2i\bar{\sigma}_l} \left(\frac{i\eta}{4} (b_l(\eta) + b_{l+2}(\eta)^*) + \frac{3f_l(\eta)}{l(l+1)(2l-1)(2l+3)} \right) \quad (\text{A.64})$$

The coefficient \tilde{S}_l^{13} behaves like l^{-3} for $l \rightarrow \infty$ and vanishes for $\eta = 0$.

The convergence of the partial wave series is quite good in general as is demonstrated in Fig. A1 for $\eta = 2$. Only $d_{11}^{[2],0}(\eta, \theta)$ shows a slower convergence at very small angles.

b. The spin-orbit contribution

According to eq. (A.34) the spin-orbit strength is given by

$$\mathbf{b} = \sum_{l=1}^{\infty} G_{LS}^l \Omega_{ll}(\hat{p}', \hat{p}). \quad (\text{A.65})$$

For the chosen reference frame, i.e. $\hat{p} = (0, 0, 1)$ and $\hat{p}' = (\cos \phi \sin \theta, \sin \phi \sin \theta, \cos \theta)$, one obtains

$$\Omega_{ll,x/y}(\hat{p}', \hat{p}) = i \frac{\hat{l}^2}{4\pi} \sqrt{\frac{6}{l(l+1)}} \begin{pmatrix} l & l & 1 \\ 1 & 0 & -1 \end{pmatrix} P_l^1(\cos \theta) \begin{Bmatrix} -\sin \phi \\ \cos \phi \end{Bmatrix}, \quad (\text{A.66})$$

$$\Omega_{ll,z}(\hat{p}', \hat{p}) = 0, \quad (\text{A.67})$$

and thus the spin-orbit vector \mathbf{b} has the form

$$\mathbf{b} = i b_0 \frac{\mathbf{p}' \times \mathbf{p}}{|\mathbf{p}' \times \mathbf{p}|} \quad (\text{A.68})$$

with

$$b_0(\eta, \theta) = -\frac{1}{2} c^{LS} \sum_{l=1}^{\infty} \beta_l(\eta) P_l^1(\cos \theta), \quad (\text{A.69})$$

where

$$\beta_l(\eta) = \frac{1}{2} \hat{l}^2 e^{2i\bar{\sigma}_l} R_{ll} = \frac{e^{2i\bar{\sigma}_l}}{l(l+1)} (2l+1+f_l(\eta)). \quad (\text{A.70})$$

This form is not well suited for a numerical evaluation, because even for $\eta = 0$ the sum extends up to infinity. Therefore, it is more advantageous to separate the η -independent part writing

$$\beta_l(\eta) = \frac{2l+1}{l(l+1)} + \beta_l^\eta \quad (\text{A.71})$$

with

$$\beta_l^\eta = \frac{e^{2i\bar{\sigma}_l}}{l(l+1)} \left((2l+1)(e^{2i\bar{\sigma}_l} - 1) + f_l(\eta) \right). \quad (\text{A.72})$$

The coefficient β_l^η vanishes for $\eta = 0$. For the η independent part one can rearrange the sum by using

$$P_l^1(x) = \frac{l(l+1)}{l^2\sqrt{1-x^2}} \left(P_{l+1}(x) - P_{l-1}(x) \right), \quad (\text{A.73})$$

and one finds

$$\begin{aligned} \sum_{l=1}^{\infty} \frac{2l+1}{l(l+1)} P_l^1(x) &= \frac{1}{\sqrt{1-x^2}} \left(\sum_{l=2}^{\infty} P_l(x) - \sum_{l=0}^{\infty} P_l(x) \right) \\ &= -\frac{1}{\sqrt{1-x^2}} (P_0(x) + P_1(x)) = -\cot(\theta/2). \end{aligned} \quad (\text{A.74})$$

Then one obtains for $b_0(\eta, \theta)$

$$b_0(\eta, \theta) = \frac{1}{2} c^{LS} \left(\cot(\theta/2) - \sum_{l=1}^{\infty} \beta_l^\eta P_l^1(\cos \theta) \right), \quad (\text{A.75})$$

yielding $b_0(0, \theta)$ in accordance with eq. (23). One can evaluate directly this expression or rearrange also the remaining sum yielding

$$b_0(\eta, \theta) = \frac{1}{2} c^{LS} \left(\cot(\theta/2) - \frac{1}{\sin \theta} \sum_{l=0}^{\infty} e_l(\eta) P_l(\cos \theta) \right), \quad (\text{A.76})$$

where for $l = 0, 1$

$$e_l(\eta) = \frac{(l+1)(l+2)}{2l+3} \beta_{l+1}^\eta, \quad (\text{A.77})$$

and for $l > 1$

$$\begin{aligned} e_l(\eta) &= \frac{(l+1)(l+2)}{2l+3} \beta_{l+1}^\eta - \frac{(l-1)l}{2l-1} \beta_{l-1}^\eta \\ &= 2e^{2i\bar{\sigma}_l} \left[i\eta \frac{2l+1}{(l+i\eta)(l+1-i\eta)} - \frac{f_l(\eta)}{(2l-1)(2l+3)} \left(2 - i\eta \left\{ \frac{2l-1}{l+1-i\eta} + \frac{2l+3}{l+i\eta} \right\} \right) \right. \\ &\quad \left. - \eta^2 \left(\frac{1}{(2l+3)(l+1-i\eta)^2} + \frac{1}{(2l-1)(l+i\eta)^2} \right) \right]. \end{aligned} \quad (\text{A.78})$$

For $l \rightarrow \infty$ the coefficients β_l^η and e_l behave as $1/l$ resulting in a considerably slower convergence than for the hyperfine amplitude. This is demonstrated for the region of small angles and near $\theta = 180^\circ$ in Fig. A2 for $\eta = 2$ for various l_{max} -values up to $l_{max} = 5000$ with the expansion of eq. (A.76). For comparison the result for the integral representation is also shown. The expansion of eq. (A.75) gives for large absolute values of η the same result. However, for small η it results in small oscillations around the result of the other expansion at small angles.

3. Comparison of the two methods

For the hyperfine and spin-orbit interactions both methods give identical results for the corresponding amplitudes as is demonstrated for the hyperfine amplitudes in Figs. A3 through A5 for $\eta = \pm 2$. The above mentioned numerical problem which arises in

the integral representation for higher negative η is illustrated in Fig. A6 where, as an example, the reduced amplitudes $\mathcal{R}_{33}^{SS}(\eta, \theta)$ and $\mathcal{I}_{33}^{SS}(\eta, \theta)$ for $\eta = 2.5$ are plotted. The two curves labeled “IR” and “PWE” are almost indistinguishable. This means also complete agreement for the amplitudes for positive $\eta > 0$ as shown in the lower two panels of Fig. A7 for the amplitude $d_{33}^{[2]}(\eta, \theta)$. Furthermore, one notes that for this η -value the two reduced amplitudes in Fig. A6 are almost equal to a high degree of accuracy. Thus, this feature creates the numerical problem mentioned above for the integral representation method, because for negative values the amplitudes are represented as differences of the reduced amplitudes (see eqs. (A.15) and (A.24)). Consequently, large cancellations occur which reduce the numerical accuracy more and more with increasing absolute values for negative η . In fact, accuracy is lost for about $-\eta > 2$. This is demonstrated in the upper two panels of Fig. A7 for $\eta = -2.5$ where one readily notes the onset of some numerical instabilities for the curves labeled “IR”, in particular at small and large angles. This limits at present the numerical application of the integral representation method.

A comparison of the two methods for the spin-orbit amplitude is shown in Fig. A8, again for $\eta = \pm 2$, where one readily notes very good agreement. The same numerical problem of the integral representation method arises also in this case for large negative η .

-
- [1] H. Arenhövel, Eur. Phys. J. A **34**, 303 (2007).
 - [2] C.J. Horowitz and H.O. Meyer, Phys. Rev. Lett. **72**, 1994 (3981).
 - [3] Th. Walcher *et al.*, Eur. Phys. J. A **34**, 447 (2007).
 - [4] A.I. Milstein, S.G. Salnikov, and V.M. Strakhovenko, arXiv:0802.3766; Nucl. Instr. Meth. B **266**, 3453 (2008).
 - [5] H. Arenhövel, Eur. Phys. J. A **39**, 133 (2009); Erratum to Eur. Phys. J. A **34**, 303 (2007).
 - [6] Th. Walcher *et al.*, Eur. Phys. J. A **39**, 137 (2009); Erratum to Eur. Phys. J. A **34**, 447 (2007).
 - [7] S.B. Levin, E.O. Alt, and S.L. Yakovlev, *Real-axis integral representation for the two-body Coulomb scattering wave function*, preprint MZ-TH/01-30 (unpublished).
 - [8] N. Dombey, Rev. Mod. Phys. **41**, 236 (1969).
 - [9] G.G. Ohlsen, Rep. Prog. Phys. **35**, 717 (1972).
 - [10] J. Bystricky, F. Lehar, and P. Winternitz, J. Phys. (France) **39**, 1 (1978).
 - [11] A. Messiah, *Mécanique Quantique* (Dunod, Paris 1969).
 - [12] U. Fano and G. Racah, *Irreducible tensorial sets* (Academic Press, 1959).
 - [13] L.C. Biedenharn and P.J. Brussard, *Coulomb Excitation* (Clarendon Press, Oxford 1965), p. 88.

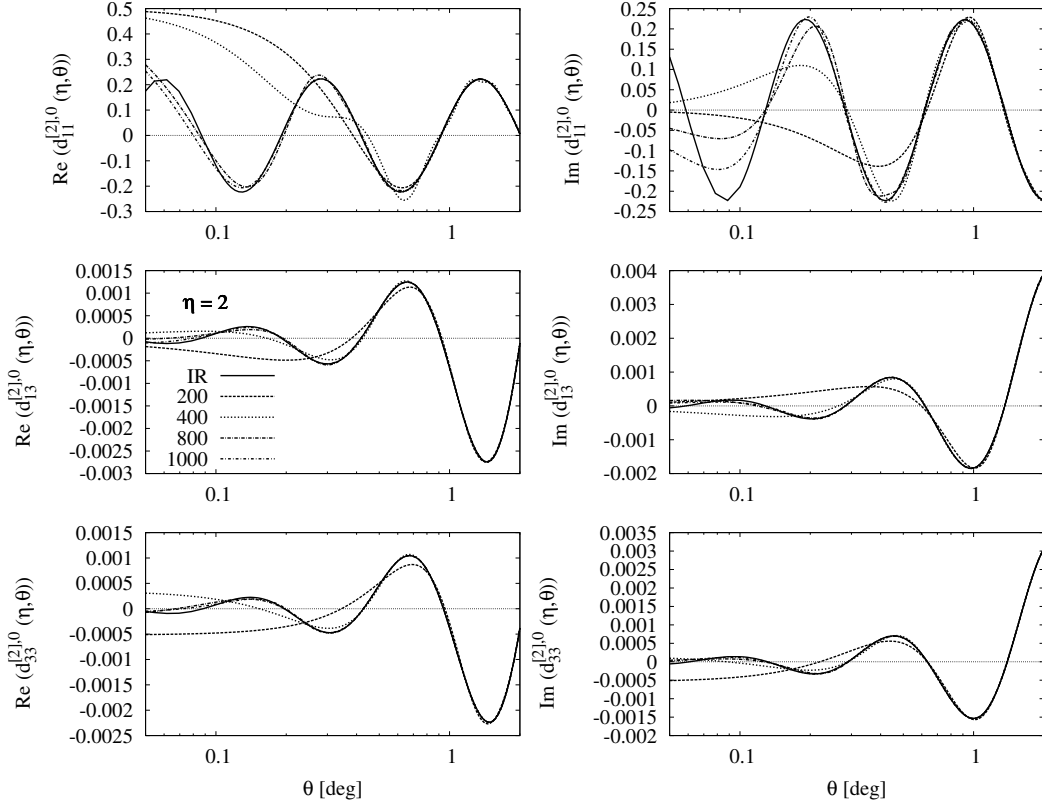


FIG. A1: Convergence of the partial wave expansion (PWE) of the hyperfine amplitudes $d_{ij}^{[2],0}(\eta, \theta)$ for various l_{max} as indicated in the legend for $\eta = 2$ for $(ij) = (11)$ (upper panels), $(ij) = (13)$ (middle panels), and $(ij) = (33)$ (lower panels). For comparison the result of the integral representation (IR, solid curves) is also shown.

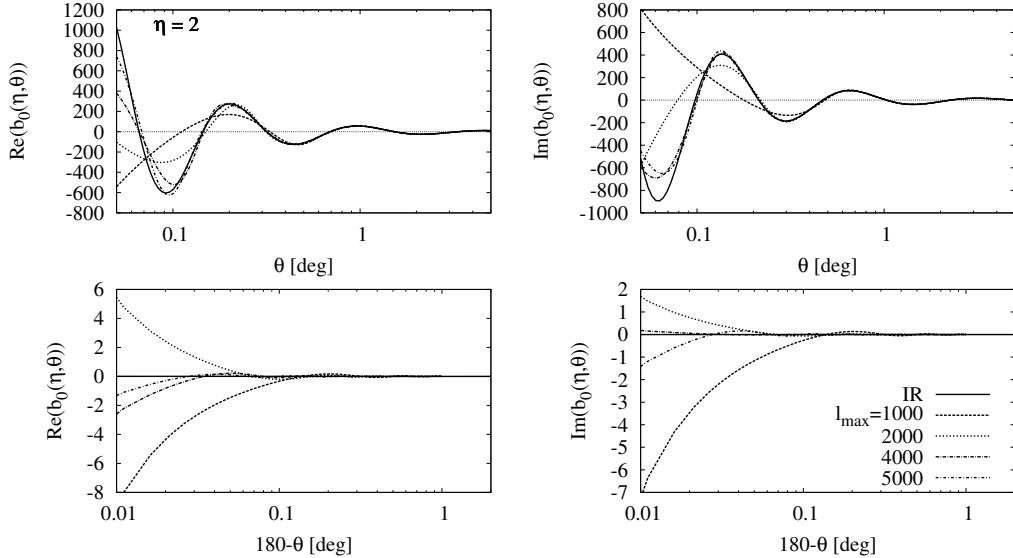


FIG. A2: Convergence of the partial wave expansion (PWE) of the spin-orbit amplitude $b^0(\eta, \theta)$ for various l_{max} as indicated in the legend for $\eta = 2$ near $\theta = 0^\circ$ (upper panels) and near 180° (lower panels). For comparison the result of the integral representation (IR, solid curves) is also shown.

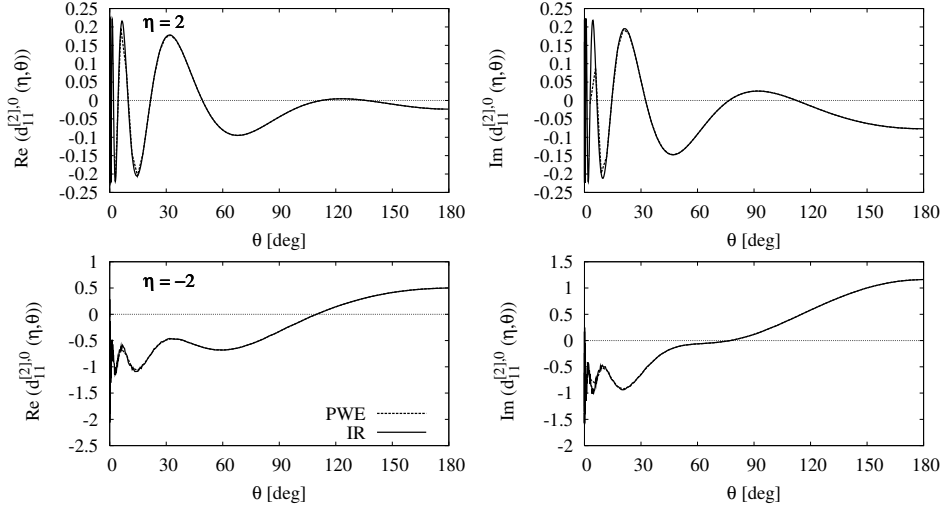


FIG. A3: Hyperfine amplitude $d_{11}^{[2],0}(\eta, \theta)$ for $\eta = \pm 2$ for the integral representation (IR) and the partial wave expansion (PWE).

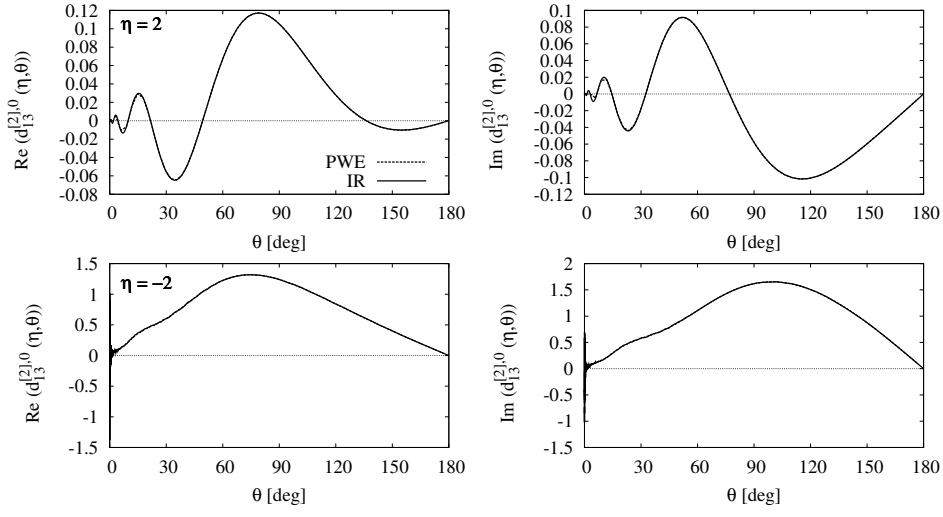


FIG. A4: Hyperfine amplitude $d_{13}^{[2],0}(\eta, \theta)$ for $\eta = \pm 2$ for the integral representation (IR) and the partial wave expansion (PWE).

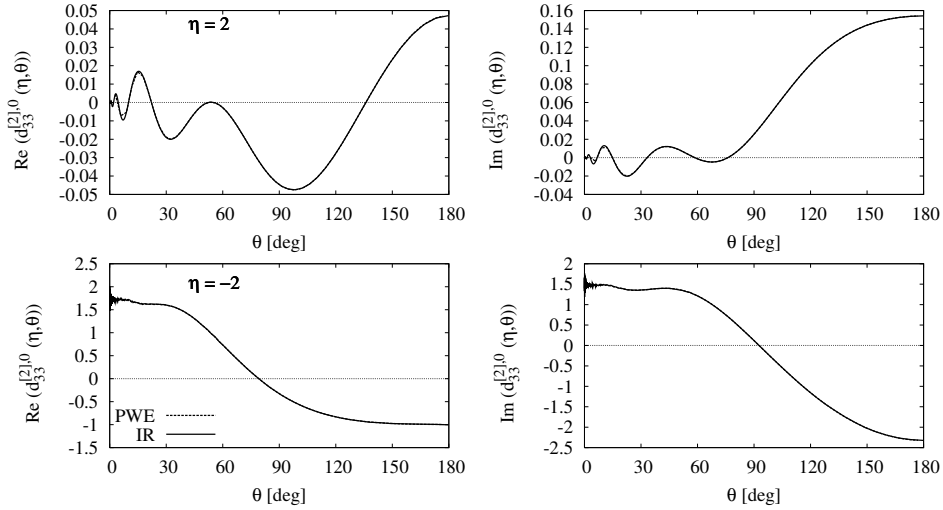


FIG. A5: Hyperfine amplitude $d_{33}^{[2],0}(\eta, \theta)$ for $\eta = \pm 2$ for the integral representation (IR) and the partial wave expansion (PWE).

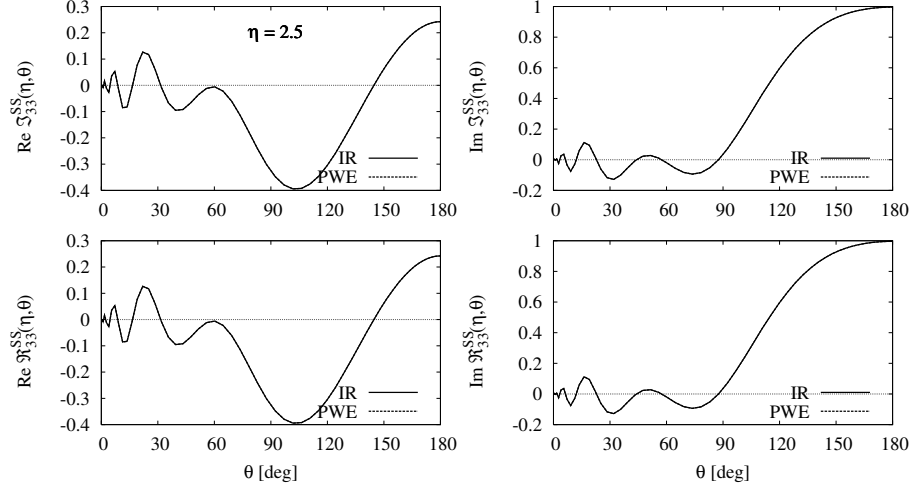


FIG. A6: Reduced amplitudes $\mathcal{R}_{33}^{SS}(\eta, \theta)$ and $\mathcal{I}_{33}^{SS}(\eta, \theta)$ for $\eta = 2.5$ for the integral representation (IR) and the partial wave expansion (PWE).

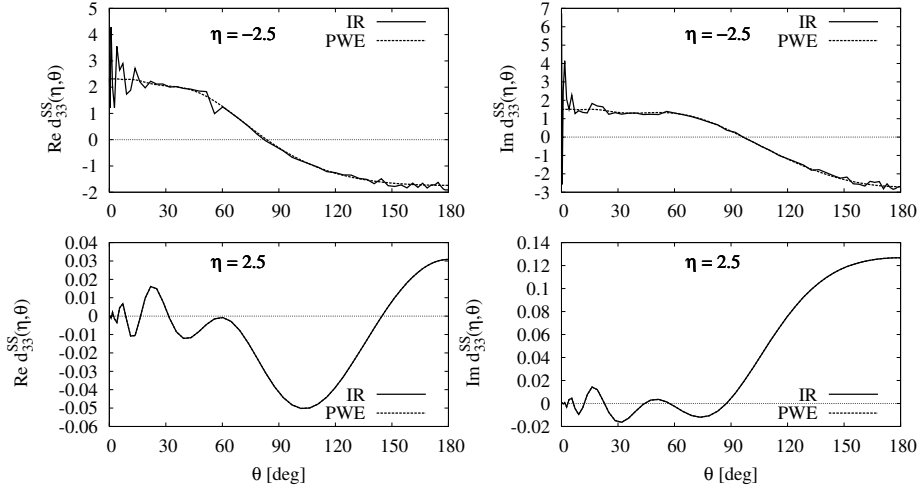


FIG. A7: Hyperfine amplitude $d_{33}^{[2],0}(\eta, \theta)$ for $\eta = \pm 2.5$ for the integral representation (IR) and the partial wave expansion (PWE).

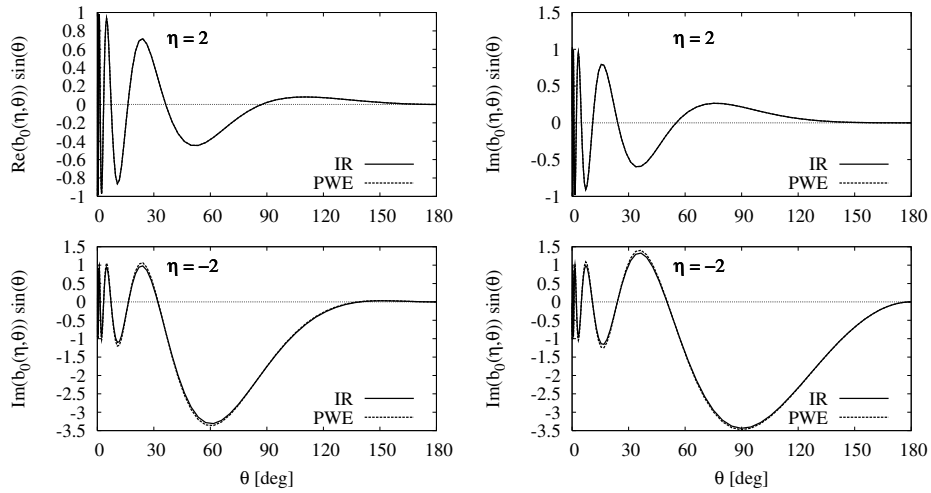


FIG. A8: Spin-orbit amplitude $b_0(\eta, \theta)$ for $\eta = \pm 2$ for the integral representation (IR) and the partial wave expansion (PWE).